AD-A053 054 HARVARD UNIV CAMBRIDGE MA DIV OF APPLIED SCIENCES F/G 20/4
FLUID MECHANICS RESEARCH.(U)
APR 78 G F CARRIER, F H ABERNATHY N00014-67-A-0298-0033

UNCLASSIFIED NL

1 OF 1
ADA
053054

END
DATE
FILMED
6-78
DDC

(12)
SC

FINAL REPORT

"Fluid Mechanics Research"

George F. Carrier

and

Frederick H. Abernathy
Harvard University
Division of Applied Sciences
Cambridge, Mass. 02138

July 1, 1971 to June 30, 1974

The research was sponsored by the Office
of Naval Research under Contract N00014-67-A0298-0033

(9) Final technical rept. 1 Jul 71 - 30 Jun 74
2

SECURITY CLASSIFICATION OF THIS PAGE (When Data Entered)

REPORT DOCUMENTATION PAGE	READ INSTRUCTIONS BEFORE COMPLETING FORM
1. REPORT NUMBER	2. GOVT ACCESSION NO. 3. RECIPIENT'S CATALOG NUMBER
4. TITLE (and Subtitle) (6) FLUID MECHANICS RESEARCH.	5. TYPE OF REPORT & PERIOD COVERED FINAL TECHNICAL 7/1/1971 -6/30/1974
	6. PERFORMING ORG. REPORT NUMBER
7. AUTHOR(s) (10) George F. Carrier and Frederick H. Abernathy	8. CONTRACT OR GRANT NUMBER(s) (15) N00014-67-A-0298-0033
9. PERFORMING ORGANIZATION NAME AND ADDRESS Division of Applied Sciences Harvard University 29 Oxford St., Cambridge, Mass. 02138	10. PROGRAM ELEMENT, PROJECT, TASK AREA & WORK UNIT NUMBERS
11. CONTROLLING OFFICE NAME AND ADDRESS ONR Dept. of the Navy Arlington, Va. 22217	(11) 12. REPORT DATE Apr 1978 13. NUMBER OF PAGES 9 (12) 48p.
14. MONITORING AGENCY NAME & ADDRESS(if different from Controlling Office)	15. SECURITY CLASS. (of this report) Unclassified
	15a. DECLASSIFICATION/DOWNGRADING SCHEDULE

16. DISTRIBUTION STATEMENT (of this Report)
Approved for Public Release; Distribution unlimited.

17. DISTRIBUTION STATEMENT (of the abstract entered in Block 20, if different from Report)

18. SUPPLEMENTARY NOTES

19. KEY WORDS (Continue on reverse side if necessary and identify by block number)
Turbulence, drag reduction, polymers, stability
Diffusion flame, Tsunamis, Wave Attenuation, Harbors,
Wave Reflection, Ocean Circulation

20. ABSTRACT (Continue on reverse side if necessary and identify by block number)
Several studies on geophysical fluid mechanical phenomena and two on diffusion flames are reported. Other ongoing but unfinished studies are listed. Experimental investigations of laminar and turbulent boundary layer flows with polymers are reported. The existence of a family of velocity fluctuations distinct from turbulence is documented.

DD FORM 1 JAN 73 1473 EDITION OF 1 NOV 65 IS OBSOLETE
S/N 0102-014-6601

410 457 JOB

FINAL REPORT

This is a final technical report for work done under Office of Naval Research Contract:

N00014-67-A-0298-0033
July 1, 1971 to June 30, 1974
"Fluid Mechanics Research"

which was a follow-on contract to N00014-67-A-0298-0002 which ended in 1971.

PART A

The work of G. F. Carrier under these contracts can best be separated in two parts:

Part I (research which has been published in the papers listed below)

Under Contract N00014-67-A-0298-0002

"Singular Perturbation Theory and Geophysics," Von Neumann lecture given at the American Mathematical Society Meeting, Aug. 23-29, 1969. SIAM Review, Vol. 12, No. 2, April 1970.

"Stochastically Driven Dynamical Systems," J. Fluid Mech., 44, part 2, pp. 249-264, 1970.

"A Model of a Mature Hurricane," (with A. L. Hammond and O. D. George), J. Fluid Mech., Vol. 47, part 1, pp. 145-170, 1971.

"The Dynamics of Tsunamis," American Math. Soc. 1970. Also in Mathematical Problems in the Geophysical Sciences, Vol. 1 - Geophysical Fluid Dynamics, William H. Reid, Editor, 1971.

"Another Useful Singular Perturbation Device," Congres International des Mathematiciens, Nice, Sept. 1970.

Under Contract N00014-67-A-0298-0033

"The Effects of Strain Rate on Diffusion Flames," (with F. E. Fendell and F. Marble), SIAM J. Appl. Math., Vol. 28, No. 2, pp. 436-500, March 1975.

"The Effect of Strain Rate on Diffusion Flames. Part II. Large Straining," (with F. E. Fendell), SIAM J. Appl. Math., Vol. 30, No. 3, pp. 515-527, May 1976.

Part II. This part consists of several studies which were initiated under N00014-67-A-0298-0033 (some completed), which have not yet been published:

(a) Wave Attenuation in Harbors. This is an effort to understand the long ringing time of Tsunami instigated waves in inlets and harbors, particularly the long (3-day) ringing of the 5-minute slashing mode in Nawiliwili Bay just after the Alaskan earthquake. This work is being continued under other sponsorship by Claude Noiseaux, a graduate student, with the supervision of Carrier.

(b) Wave Reflection by Irregular Topography. This completed effort provided a reasonably efficient way of calculating the reflection of gravity waves by an irregular bottom contour. It also arose in connection with Tsunami propagation but, until a specific application seems to merit a detailed application, publication is not likely to arouse much interest.

(c) The Mid-Latitude Ocean Circulation. For many years, those who study models of the wind-driven, mid-latitude circulation have failed to treat successfully the steady (but unstable) state corresponding to the most interesting Rossby number range. A new formulation and an appropriate (classical) technique have yielded very encouraging preliminary results and this work is continuing under other sponsorship.

(d) During a sabbatical visit to Harvard by Wilbert Lick of Case-Western Reserve, he and Carrier tried to model the dynamics, thermo-dynamics and heat transfer mechanisms which are important in Cumulo-Nimbus activity. The work was instructive but no definitive results were obtained. The insight gained has been useful in other studies but no publications of this work, in its own right, seemed justified.

(e) During the spring term of 1971-72, Leon Knopoff's visit to Harvard had ONR support (letter report by G. F. Carrier of June 15, 1973). His pub-

lication "The Dynamics of a One-Dimensional Fault in the Presence of Friction," Publication No. 1166, Institute of Geophysics and Planetary Physics, University of California, Los Angeles was an outgrowth of that visit.

PART B

The work of F. H. Abernathy under this contract can be divided into separable though interconnected activities. The first activity was the development of a technique for using laser-Doppler anemometry in high strain rates flows. The second activity was a detailed investigation of the mixing in a turbulent boundary using drag-reducing polymers to selectively inhibit motions based on their strain rates. Both of these activities were initially supported under this contract, with continuing sponsorship provided by NSF.

The work performed under both activities has been published:

(1) "Turbulence Spectra Using Laser-Doppler Anemometry and Selective Seeding," F. H. Abernathy, J. R. Bertschy, and R. W. Chin, Biennial Turbulence Conference, University of Missouri-Rolla, Oct. 1977.

(2) "Modifications to Laminar and Turbulent Boundary Layers Due to the Addition of Dilute Polymer Solutions," J. R. Bertschy and F. H. Abernathy, BHRA Fluid Engineering, Second International Conference on Drag Reduction, Cambridge, England, August 1977.

Both of these papers will be available in the proceedings of these meetings. For convenience, a copy of each paper is attached to this report in Appendix I-a, and Appendix I-b, and briefly summarized as follows:

Using the selective seeding technique described in (1) above, it is possible to obtain thousands of velocity determinations per seconds in water shear flows with spatial resolution of the order of 25 μ. A plane of hydrogen bubbles is generated by electrolysis from a wire upstream of the laser-Doppler scattering volume. The intersection of the plane of bubbbles with the scattering volume becomes the major source of scattered light if the flow is prefiltered. This technique requires a relatively simple correction for velocity determinations. The correction is necessary because the bubbles are in the wake of the generating wire. The bubble generation rate can be controlled. At the upper limit a hydrogen bubble is nearly always crossing the scattering volume. The laser-Doppler output then is nearly a continuous time signal. Hence the laser-Doppler signal can be time averaged, frequency filtered, etc. Power spectural density measurements can be made in flows where it would have been impossible before the technique was developed. It also makes it possible to obtain detailed velocity profiles of flows which would have been impossible to obtain by other means. It is felt that this technique will become useful in a variety of flow situations.

The addition of polymers in dilute concentrations to laminar and turbulent boundary layer causes significant effects. What has been called "early turbulence" by others has been shown to be not turbulence but rather fluctuations in the laminar layer, probably associated with the relaxation time of the polymer itself. Using the selective seeding technique, it has been possible to analyze the spectrum of the fluctuations and show that they are distinct from turbulence. In addition as polymer

concentration and strain rate increase, the difference between laminar and turbulent layers disappears. Implications of these results are under active investigation.

PART C

Under this contract a substantial research effort on "Grid Turbulence in a Liquid System" was undertaken by Carol Russo under Professor Howard W. Emmons.

The final work on this experiment was completed in May of 1975. At the same time a Ph. D. thesis was written and accepted entitled, "An Experimental Study of Grid Turbulence in a Liquid". A copy of the thesis synopsis is attached which summarizes the entire effort on this project and draws conclusions.

SYNOPSIS

Measurements were made of the intensities and of the transverse and longitudinal double correlations of grid turbulence in the initial region of decay in methanol to verify for a liquid the theoretical and semi-empirical equations for isotropic turbulence that have been previously verified in air. This experiment was undertaken primarily for two reasons. First, some question of the validity of these equations for a liquid was raised by Tan and Ling's intensity data taken behind a grid in water because their intensities were much higher than those measured in air under apparently equivalent experimental conditions. It was not clear whether the differences in molecular structure between gases and liquids which change the mechanisms involved in diffusion processes would effect the basic equations describing the behavior of isotropic turbulence. Secondly, it became clear in the air data that changes in the mean speed U and the mesh size M which partly comprise the mesh Reynolds' number (UM/ν), the primary similarity parameter, did not equally effect the resulting intensity. It seemed important to determine if changing the kinematic viscosity would significantly effect the properties of the grid turbulence. The experiments in air could not vary the kinematic viscosity over a large range. Using a liquid instead of a gas is a simple way to dramatically vary the kinematic viscosity.

Measurements of both intensity and correlation were in general in good agreement with the experimental results found in air. The grid turbulent energy decayed linearly with distance with slopes equal to those in air. The turbulent intensity reacted to changes in similarity parameters such as mesh to wire diameter ratio and mesh and wire diameter Reynolds' numbers in a manner similar to that found in air. Also, the intensities in methanol fell within the zone of scatter of the air data. However, detailed comparisons

of the values of the grid turbulence intensities show differences much larger than known experimental errors and which cannot be explained by the differences in factors such as the free stream turbulence. For the same values of the similarity parameters Re_M, M/d, and x/M, the intensities in methanol were lower than those found in air. The lateral and longitudinal double correlations were in good agreement with those measured in air also. The correlations measured in methanol were also in agreement with the purely theoretical equation relating the lateral and longitudinal correlations for isotropic turbulence which shows that in methanol grid turbulence is also isotropic. In contrast to the grid intensities, the behavior of the correlations is well explained in detail by the usual similarity parameters in both methanol and air.

It is clear that while the general behavior of grid turbulence has been given by the theoretical and semi-empirical equations verified in air, some of the parameters needed to predict the value of the intensity precisely remain to be found. It would require an experiment much more extensive and with smaller experimental errors to unravel the details of grid turbulence behavior.

Second International Conference on

Drag Reduction

August 31st - September 2nd, 1977

PAPER G1

MODIFICATIONS TO LAMINAR AND TURBULENT BOUNDARY LAYERS DUE TO THE ADDITION OF DILUTE POLYMER SOLUTIONS

J.R. Bertshy and F.H. Abernathy,

Harvard University, U.S.A.

Summary

Two-dimensional boundary layer flows of dilute solutions of Polyox, WSR-301, have been investigated on a free surface water table. The natural disturbance level was low enough so undisturbed water flows were laminar. The flows had wall shear velocities up to 4.2 cm/sec and were at concentrations up to 32ppm as determined by testing samples in a vortex viscometer. Observations were made of the free surface, injected dye, streak spacing and the time-dependent velocity in the mean flow direction as a function of polymer concentration, wall strain rate and disturbance. Nearly continuous and very localized velocities were measured using a laser-Doppler anemometer and a novel method of selective seeding. Velocity spectra were also obtained.

Undisturbed polymer flows at sufficient concentration and strain rate exhibited velocity fluctuations distinct from turbulence. We have termed these as polymer induced fluctuations and believe that they are most likely responsible for the phenomenon of so called "early turbulence". Studies of turbulent polymer flows (disturbed artificially) indicated significant drag reduction and were all consistent with the view that hairpin eddies are the major mixing mechanism in a turbulent boundary layer, and that these eddies are suppressed by the addition of polymers. When strain rate and/or concentration were increased somewhat, polymer fluctuations were found to coexist with the turbulent motions. At still higher strain rates and/or concentrations, the polymer fluctuations dominated and the turbulent flow reached suppressed condition. No distinction between artificially disturbed and undisturbed flows at the same conditions could be observed.

Held at St. John's College, Cambridge, England.
Organised and sponsored by BHRA Fluid Engineering, Cranfield, Bedford, MK43 0AJ.

NOMENCLATURE

u = time dependent velocity in the mean flow direction

u'^+ = rms fluctuating velocity divided by u_τ

U^+ = mean velocity divided by u_τ

u_τ = wall shear velocity

y^+ = $y\, u_\tau/\nu$, y = distance from the wall ν=solvent viscosity (water)

λ^+ = $\lambda u_\tau/\nu$, λ = mean streak spacing

INTRODUCTION

The turbulent drag reducing capability of dilute polymer solutions has been known for a number of years. The two review articles by Lumley (ref. 1,2) and the extensive surveys of Hoyt (ref. 3) and Virk (ref. 4) review and place in perspective the known aspects of dilute polymer flows. Yet, mechanisms by which the turbulent mixing is reduced are still poorly understood. For example, Rudd (ref. 5), Logan (ref. 6) and Kumor and Sylvester (ref. 7) have each reported that the magnitude of the fluctuation component of the velocity in the mean flow direction, u'^+, in a turbulent boundary layer very near the wall increases with the addition of polymers. This has been interpreted as the polymers working primarily to thicken the viscous sublayer. On the other hand, Reischman and Tiederman (ref. 8) have reported a decrease in the maximum intensity of u'^+ near the wall and (along with ref. 9) found a broad peak from $y^+ = 25$ and beyond. They have interpreted this as an indication that polymers in drag reducing flows primarily alter the buffer zone (ref. 4). They reported finding no indication of a thickening of the sublayer. The present investigation was designed to explore the cause of these observed velocity fluctuations in dilute polymer boundary layers and to determine in what ways they differed from those observed with Newtonian fluids.

At the beginning of the present investigation, we held the view that the major turbulent mixing mechanism near a solid boundary was due to three-dimensional flows induced by hairpin eddies aligned in the flow direction. The addition of dissolved polymers to the flow should inhibit the formation and hence the mixing arising from such vortex pairs. At high enough polymer concentrations, the flow near the wall should be essentially laminar. The results of our experiments required only minor modification of this initial view of the turbulent boundary layer.

The experiments were designed to investigate boundary layer flows, at high enough Reynolds numbers to achieve turbulence if artificially disturbed, but at low enough free stream disturbance levels to enable a laminar boundary layer flow to exist in the absence of such disturbances. This enabled us to observe what, if any, velocity fluctuations might arise from the polymers themselves.

A free surface water table was selected as the optimal flow apparatus. In addition to fulfilling the prerequisites mentioned above, this apparatus is well suited for optical probing, since all surfaces are planar and the flow is easily accessible. The water table also has the tremendously useful benefit of providing information concerning where and when transition to turbulence or some other unsteady flow has occurred by visual observation of the free surface.

EXPERIMENTAL FLOW ARRANGEMENT AND EQUIPMENT

A diagram of the flow arrangement is shown in Fig. 1. Basically, filtered tap water is pumped from a sump reservoir through an overflow standpipe to a water table inclined to the horizontal. It then returns to the sump via a weighing tank. Polymer solutions were injected for short periods. It has been assumed that the polymers have been severely degraded before they return for a second time to the water table, especially since a large depth filter (5μ nominal pore size) was interposed in the flow circuit. In addition, the sump reservoir is so large (approximately 17,000ℓ)

that effects of polymers returning for a second pass were neither expected nor observed. Concentrated (200-500 ppm) polymer solutions were injected by gravity feed from constant pressure tanks (two 208ℓ drums) into the piping over 38 diameters from the water table. Thus, the final dilution to the test concentration was accomplished by turbulent mixing in this pipe (10 cm dia.).

The water table has a deeper inlet section equipped with large cell honeycomb flow straighteners and surface wave calming devices. There is a smooth transition to the glass working section which is 1.22m x 1.83m. Typically, the flow was run 1.9 to 3.5 mm deep and the table's inclination was from 1.6^{o} to 4.2^{o}. All undisturbed water flows presented in this paper were laminar. To trip this flow to turbulence, a bead-chain of 2.63 mm beads was inserted in the flow near the leading edge of the glass working section.

Velocity measurements were made using a LDA manufactured by Thermo Systems, Inc. (TSI) oriented as shown in Fig. 2. The laser used had a 1 mW polarized output. Signal processing was accomplished by a TSI model 1090 tracker. It is normally difficult to resolve the local velocity in a thin shear flow using LDA techniques since the scattering volume of the intersecting laser beams is relatively large (here, 0.15mm dia. by 1.7mm length). We have overcome this difficulty by introducing light scattering contaminants to the flow only at a selected distance from the wall. This is accomplished by generating bubbles by electrolysis from a fine wire held parallel to the wall and normal to the flow. Most other scattering particles are filtered out of the flows. Hence, using a forward scatter, fringe mode LDA with the long axis of the scattering volume normal to the wall, we can obtain laminar and turbulent velocity profiles relatively rapidly by moving the bubble generating wire normal to the wall (cf. Fig. 2).

The bubble wire used was 80%Pt20%Ir, 0.0025 cm in diameter and 5 cm long. It was supported across two insulated, L-shaped, stainless steel tubes which entered the flow downstream of the scattering volume. The wire was always positioned at least 300 diameters upstream of the scattering volume so that its wake would not be detected (ref. 10). The flow was always such that the local Reynolds number of the wire was less than 25, so instability of the wire wake was never a problem. By adding a salt to the water (Na_2SO_4, anhydrous) we were able to maintain a sufficiently high bubble production rate so that the measured velocity was practically continuous (from 1000 to 6000 velocity samples/sec.) while the operating voltage was reasonably safe (<300V).*

To obtain mean velocities and rms turbulent intensities, a signal analysis box developed at the lab was used. It measured the mean voltage of the tracker's output by a continuously integrating op-amp with an accuracy of 0.1%. This voltage was electronically subtracted from the tracker output and then fed to a Burr-Brown 4128 rms module which determined true rms of this difference. Its accuracy is about 0.3% from 0.1 Hz to 20 kHz. Readings were taken using a 3½ digit Data Precision digital multimeter. Due to the one-pass nature of the experiments, short time constants were used and the measurements were considerably more uncertain than the potential accuracy of this instrumentation.

Velocity spectra were taken using a Tektronix 7L5 Spectrum Analyzer. It operates digitally and was set to filter with a 10 Hz bandwidth. Since it could not accept a dc signal from a high impedance source, a capacitor coupled op amp of gain 1 was interposed between the tracker and the spectrum analyzer.

Depth measurements were taken using a needle, point gauge accurate to 0.001 cm for flows with a smooth free surface. The water table's inclination was monitored by a 254 cm long liquid level located along the table side. A thermometer in the stilling section read temperature with an accuracy of 0.1^{o}C.

---

* Cambridge City water contains typically 100-150 ppm of dissolved salts. The addition of 100-150 ppm of Na_2SO_4, to increase the electrical conductivity, did not effect the occurrence of polymer induced fluctuations as determined by viewing the free surface. While no quantitative measurements of the dependence of polymer effects on salt concentration were made, we have no evidence to suggest the results were influenced by the salts.

Polymer Preparation and the Rheological Test of Concentration

Batches of 0.1% solution (15ℓ) of PEO, WSR-301, were prepared by sprinkling the dry powder on the surface and hand mixing gently with a large paddle. This solution was allowed to sit for two days before using. The dry polymer was not dispersed in an alcohol slurry since the flow over the water table is shallow enough that it might be sensitive to surface tension changes. Surface tension measurements indicated that polymer solutions of much higher concentrations than those used in the water table exhibited negligible deviation from that of water.

The polymer concentration of a given flow was determined by withdrawing a sample during each run and observing its behavior in a large scale vortical flow similar to that of Balakrishnan and Gordon (ref. 11). They have demonstrated that measuring the minimum polymer concentration needed to achieve "vortex inhibition" is a more sensitive test for degradation than intrinsic viscosity measurements. So, we used a modified form of their bathtub vortex experiment as a rheological test for polymer concentration. Briefly the procedure was as follows: 20ℓ of the fluid to be tested was placed in a cylindrical container (29.2 cm inside dia.) with a central drain. The container was rotated until solid-body rotation was achieved (50 rpm) and then quickly stopped. Draining was commenced immediately and the vortex was allowed to form under the maximum draining rate. The drain was connected to a long flexible tube whose outlet elevation could be freely varied.

Since nearly all the flows we ran over the water table had concentrations below "vortex inhibition" (25 ppm for WSR-301) the air-liquid interface reached to the drain and there was two-phase flow in the exhaust tube. As soon as the vortex was securely established, the end of the exhaust tube was raised until two-phase flow no longer occurred in it. This elevation was then compared to a calibration curve made using dilute solutions made from a single batch of 0.1% stock solution. Thus, we were able to judge the concentration compared with this single stock solution to about 2 ppm independently of how poorly prepared or mishandled the sample had been. Typically, samples after passing over the water table behaved in the vortex as if their concentration had been 25% to 50% less than that injected.

The effective concentration of polymer determined by the vortex viscometer was in agreement with the water table flow observations. All data is presented with the concentration as determined in this fashion. In the near future, we expect to undertake a detailed study of this vortex flow.

Velocity Data

In so far as time allowed, complete profiles of u-velocity and turbulence intensity, were measured for each polymer run (45 minutes or less). Since the LDA would occasionally lose track of the Doppler signal, only short time averaging (about 8 sec.) was possible to ensure quick recovery. In addition, bubble production was reduced in polymer flows so constant attention was necessary to obtain data.

All velocity and depth measurements were taken at a station 146 cm downstream of the transition from the stilling section to the test section. Since the flows were typically 0.2 cm to 0.3 cm deep, this corresponds to a test location between 730 and 500 flow depths downstream of the transition.

Wall shear stress and hence u_τ was inferred from the depth measurement and the table inclination and assuming flow equilibrium. The flow accelerates as it progresses down the table and wall shear stress accordingly increases. A turbulent water flow comes to an equilibrium depth (and hence velocity) within 60 cm on the flat test section, while laminar water flow has not quite come to equilibrium even at the measuring station 146 cm downstream. Estimates of the acceleration of laminar water flows similar to those in which polymers were tested indicate that at most, u_τ might be decreased by 4% from the value used. Flows indicating any fluctuation and hence an increase in momentum exchange from laminar water flows were certainly much closer to equilibrium. Uncertainty in depth and angle measurements lead to an uncertainty in u_τ of $\pm$ 0.02 cm/sec for laminar flows and $\pm$ 0.06 cm/sec for turbulent flows.

The position of the bubble wire relative to the wall was also determined by the depth and angle measurements. Average velocity data from a laminar flow was plotted with relative uncertainty in position of only $\pm$ 0.001 cm. The wall shear stress measure (assuming solvent kinematic viscosity) was then used as an indication of the slope this velocity data had to have at the wall. The two were then compared and an absolute measure of distance from the wall to the bubble wire was determined with an uncertainty of approximately $\pm$ 0.005 cm.

All data is presented using the solvent kinematic viscosity as determined by the temperature. There is evidence that this may not be the best method to correlate the data; however, most previous investigators have presented their data using solvent viscosity. We do so to facilitate comparison, but point out that Reischman and Tiederman (ref. 8) did not follow this practice and allowances should be made accordingly.

One further flow visualization experiment was performed to obtain the streak spacing. Grains of Na_2SO_4 were sprinkled into the flow. Since the salt is denser than water, it tended to travel downstream along the bottom glass wall of the water table. The grains are small enough, however, to be lifted by turbulent motions and streaks were readily observed. Since the terminal velocity of these salt grains in still water is about 1 or 3 cm/sec, it is likely that the turbulent motions must occasionally exceed this velocity for streaks to be detected in this manner.

EXPERIMENTAL RESULTS

The philosophy used throughout this investigation has been to compare the dilute polymer flows with those of pure water at comparable strain rates and depths of flow. Following such a program required a careful investigation of the flow of water, measuring all of the variables with the same techniques to be used with dilute polymer flow.

The dimensionless mean velocity U^+ is plotted versus dimensionless distance away from the wall y^+ for both laminar and turbulent flow of water in Fig. 3. The measured results for the turbulent boundary layer flow of water show very close agreement with the "law of the wall" results for Newtonian fluids from both boundary layer and pipe flow. In fact, the water table turbulence data is nicely bracketed by the extremes commonly quoted in the literature for this universal profile (ref. 12). Departure from the universal velocity profile naturally does occur near the free surface since the slope $\frac{dU}{dy}$ must go to zero there. The laminar profile is a reasonable approximation to the calculated asymptotic limit. The nondimensional rms value of the fluctuating component of u velocity, u'^+ is plotted in Fig. 4 for turbulent water flow along with the laminar value, which results from the noise level of the LDA. (All u'^+ values presented have been corrected for this level.) The general shape and the location of the peak of u'^+ at $y^+ = 15$ conforms with the published measurements (ref. 12); however, the overall scale of u'^+ is lower for the water table flow. This should be expected because the water table flow extends only to y^+ on the order of 100, while pipe flow and boundary layer flow generally have a log layer flow several orders of magnitude larger. The limited log layer of water table flow does not effect the mean profile (Fig. 3) nor the shape of u'^+, it only decreases the latter's scale.

The mean and fluctuating velocity profiles for water (Figs. 3 and 4) were obtained using the selective seeding LDA technique. Nearly continuous velocity measurements can be frequency analyzed, and Fig. 5 shows the oscilloscope output from the spectrum analyzer at $y^+ = 14$, 48 and 58 for a water turbulent boundary layer. These three values of y^+ are in the neighborhood of those that will be presented for polymer flows. The fluctuations in spectral intensity are due to the manner in which the analyzer operates. Its 10 Hz pass band slowly and automatically sweeps across the frequency range of 0 to 500 Hz. When centered at a particular frequency, the signal then entering the instrument is digitally analyzed. Successive averaging of such spectra would naturally decrease the fluctuations in Fig. 5, resulting in a smooth curve over the 0 to 500 Hz range. The three spectral traces in Fig. 5 show no major variations from $y^+ = 14$ to $y^+ = 54$, suggesting that the same disturbances are active throughout the buffer layer. A large fraction of the fluctuation is at low frequency,

below 75 Hz. Assuming these fluctuations are convected with the local velocity suggests that their wavelength is greater than the thickness of the layer, which is verified by visual observations of the free surface.

The object of the experiments was to determine how polymer concentrations and wall strain rate modify laminar flows and then to induce transition to turbulence and again measure the same parameter dependence. Since the wall shear stress as of turbulent and laminar flow at constant mass flow and table inclination differ in general, a patch of turbulent flow will be deeper than a laminar region and therefore easily seen by looking at the free surface (Fig. 6a). It was this property which led to the discovery by Emmons (ref. 13) of spots on a water table. Such spots can be reproducibly generated by injecting a pulse of fluid from a hypodermic tube upstream of the entrance contraction. The injected fluid creates a three-dimensional disturbance (mostly a vortex ring) which triggers a localized transition to turbulence. The spanwise extent of the turbulence is many times the depth of the flow. In water the width of the spot along the span increases as the spot is convected downstream. Recently (ref. 14) spots in an air boundary layer have been studied and the velocity profile in the spot away from the leading and trailing edges has been found to be fully turbulent.

With the addition of polymers to the flow, spot formation is altered dramatically (Fig. 6b). In contrast to a spot in pure water the lateral growth rate is greatly reduced and the depth of a spot is not much different from the laminar flow surrounding it. As the shear stress or polymer concentration increases, fluctuations on the free surface of the otherwise laminar flow appear and can be seen in the background flow of Fig. 6c. These fluctuations are distinct from those due to turbulence, since transition to turbulence can still be induced (Fig. 6c). An increase in wall shear (above the laminar value) in pipe flows at Reynolds numbers below the expected turbulent transition has been observed (ref. 15) and this was called early turbulence. It appears likely that this increase in drag can be attributed to the velocity fluctuations visible in Fig. 6c. We have called these velocity fluctuations polymer induced fluctuations because they differ from turbulence. The distinction between polymer induced velocity fluctuations in laminar flow and turbulence fluctuations is sharp at moderate concentrations and strain rates and becomes less distinct at higher concentrations and strain rates. Hence, it will be important to distinguish between laminar-like properties and turbulent-like properties. For laminar flow:

(1) The free surface is smooth and free of waves (background of Fig. 6a, away from the spots).

(2) The u-velocity trace is relatively smooth; its spectrum is broadband, and u'^{+} is low and essentially independent of y^{+} (Fig. 4).

(3) Dye introduced at the wall is convected along the wall with little lateral spread; salts introduced in the flow show no evidence of streaks.

(4) By introducing disturbances, either by a trip cord or by injecting fluid, an instability can be generated which causes transition to turbulence.

(5) The mean velocity profile can be distinguished from the turbulent profile (Fig. 3 for water).

For turbulent flow:

(1) The free surface is wavy with many wavelengths greater than depth (the spot in Fig. 6a).

(2) The u-velocity has a large fluctuating component (Fig. 4) and spectra (Fig. 5) have large low frequency components and are essentially independent of y^{+}.

(3) Dye introduced at the wall is rapidly dispersed; salts introduced at the wall give evidence of streaks with a spanwise spacing (λ^{+}) of 116 ± 15.

(4) Introducing disturbances has no noticeable effects on the flow downstream of the disturbance.

(5) The mean velocity profile follows the universal velocity distribution for turbulent flow (Fig. 3).

Laminar Flow with Polymers

Laminar flows with dissolved polymers exhibit fluctuations on the free surface only for certain values of concentration and wall strain rate (dU/dy), as shown in Fig. 7. No attempt was made to define the region precisely as it was enough for this initial investigation to determine the general boundaries of the region. The form that this boundary curve assumes is consistent with observations for the onset of drag reduction. Berman and George (ref. 16) suggest a time scale criterion which for WSR-301 predicts an onset strain rate of about 320 sec^{-1}*, certainly less than the strain at the knee 720 sec^{-1} of Fig. 7. While drag reduction has been observed near the limit of infinite dilution, the onset strain rate increases as concentration decreases (ref. 17). This too is in accord with the trends of Fig. 7, suggesting that polymer fluctuations are closely related to the mechanisms of polymer drag reduction.

Graphs of u'^+ vs y^+ for polymer fluctuations at several strain rates and concentrations are shown in Fig. 8. At first glance, they are similar to those for water turbulence in Fig. 4. For all cases except for the highest concentration and strain rate, u'^+ peaks at $y^+ \simeq 15$ and then falls off to a much lower value at higher y^+. The strong difference between the polymer fluctuation and water turbulence can be seen in the spectra shown in Fig. 9 which correspond to conditions 2 in Fig. 8. These spectra show the features common to all cases of polymer fluctuations, namely strong spectral variation with y^+ while the low and high frequencies are suppressed compared to water turbulence. Compared to laminar flow of water, there is the addition of fluctuating components in the 50 Hz to 150 Hz range. With these fluctuations confined in a region around $y^+ = 15$, it is natural to assume they are convected with the local mean velocity implying a wavelength on the order of the layer thickness or larger. An inspection of the free surface (cf. Fig. 6c) shows wavelengths on the order of the layer depth. It is a characteristic of laminar layers with polymer fluctuations to have the more intense fluctuations confined to a region near the wall. As either the concentration or strain rate increases, the vertical extent increases, out to $y^+ \simeq 35$ at the highest strain rate and concentrations tested. In all cases the polymer fluctuations as detected in u'^+ were in the frequency range of 50 to 150 Hz and could be detected only near the wall (cf. Fig. 10). In addition, it appears that u'^+ at large y^+ tends to increase with concentration.

The mean velocity profiles U^+ versus y^+ were quite sensitive to polymer concentration. The velocity curves 1 and 2 in Fig. 10 correspond to conditions 1 and 3 on Fig. 8. At lower concentration, for example 13 ppm, where polymer fluctuations can first be detected, the measured profiles fall between water laminar and curves 1 and 2. If the mean velocity curves had been corrected for the kinematic viscosity's dependence on polymer concentration and strain rate, then the profiles would have fallen closer to the water laminar curve. The measured mean velocity profiles for polymer fluctuations are similar to those of the laminar flow of water, with an apparent higher viscosity. This holds true up to effective polymer concentrations of 25 to 32 ppm where it is impossible to distinguish between polymer fluctuations and polymer turbulence if the strain rate is high enough for polymer effects to be observed (cf. Fig. 7).

For flow described as polymer fluctuations, attempts were made to find evidence of streaks in the flow direction but none were observed. For water turbulence, streaks were observed, and their mean spacing in dimensionless wall variables was 116 ± 15, in agreement with measurements in air and water of many others using many different techniques.

Turbulent Flows with Polymers

The same type of experiments and measurements already reported for the polymer fluctuations were repeated for turbulent flows. It was necessary to introduce a

*Berman and George (ref. 16) used WSR-N80 and determined onset for glycerine-water polymer solutions. We have adjusted their value to account for the higher molecular weight and intrinsic viscosity of WSR-301 to arrive at this figure for onset.

larger disturbance to cause transition to turbulence at higher polymer concentrations than it was for pure water transition. The larger disturbances were either longer time pulses of fluid to cause transition in spots (cf. Fig. 6b) or larger diameter rods that spanned the flow at the entrance station. Hansen et al (ref. 18) on the basis of a linear stability analysis of pipe flow, using a single time scale viscosity model for dilute polymers, calculated that the growth rate of disturbances would be altered by the polymers. From our observations of the water table flows, we can report that larger amplitude disturbances are definitely necessary for transition, and that the spanwise growth of turbulent spots is also greatly reduced. In fact, three-dimensional spanwise variations in disturbances appear to be required to insure reproducible turbulent flow. A bead-chain (in fact an aluminium electric light pull chain) was used which completely spanned the flow at the entrance station. The bead-chain seemed satisfactory for all flows. Observations were made of the free surface with and without the chain. Additional disturbances such as cylinder 2 or 3 cm in dia. placed in the flow downstream of the chain resulted in no observable effects for more than a few diameters. It was therefore concluded that turbulent conditions with polymers had been achieved, and it is this condition which was used for the reported flow measurements.

The visual appearance of free surface is different for polymer turbulence and polymer fluctuations at concentrations below 25 ppm as can be seen in Figs. 6b and 6c. The amplitude and wavelength of the free surface fluctuations are much larger for turbulence than for polymer fluctuations, as the spectrum of u'^+ reveals. In addition, the turbulent patch is deeper than the surrounding flow since the wall shear stress under the patch is greater.

The measurements of u'^+ vs y^+ for several polymer concentrations and strain rates are plotted in Fig. 11 along with that of pure water for reference. At the lowest concentration there is an increase in the magnitude of u'^+ over that of pure water, even though the spectral distribution (Fig. 12) is quite similar to that of pure water. At this concentration, no polymer fluctuations were detected in the laminar flow. Curve 2 in Fig. 11 shows a double peak in intensity, and its u-velocity spectra at four different values of y^+ are shown in Fig. 13. The first peak near $y^+ = 15$ appears to be associated with polymer fluctuations both on the basis of its y^+ location and the u-velocity spectrum. The increase in spectral intensity at lower frequency is definitely present. The second peak near y^+ of 30, on the basis of the spectra at $y^+ = 32$ and 41, is probably associated with the turbulence process.

From the wide range of the u'^+ versus y^+ data as a function of polymer concentration and strain rate, it is apparent that a simple characterization of the fluctuation dependence is not possible. Our results for a two-dimension mean flow indicate a strong dependence on wall strain rate over the entire range of polymer concentration from low to intermediate, and to high. Curve 1 of Fig. 11 indicates that u'^+ is augmented over the solvent values at low concentrations; curves 2, 3 and 4 are all for a moderate concentration of~16 ppm and show the richness of the strain rate dependence. The lower strain rate (curve 3; $u_\tau = 3.25$ cm/sec) has u'^+ below the solvent value for all y^+. The u velocity spectra at the next highest strain rate ($u_\tau = 3.52$ cm/sec) in Fig. 13 shows evidence of strong polymer fluctuations near $y^+ = 15$, the first peak in the u'^+ intensity. Increasing u_τ to 3.85 cm/sec lowers the intensity of u'^+ everywhere, the spectrum near the peak shown in Fig. 14 being suggestive of polymer fluctuations. Curves 5 and 6 of Fig. 11 are representative of what we have called asymptotic conditions or suppressed turbulence. The effective concentrations and strain rates are so large that no distinction can be made between the flow with and without the bead-chain disturbance. Spectra for curve 5 of Fig. 11 are shown in Fig. 15. The flow is inactive except for the fluctuations near the wall which which are suggestive of polymer fluctuations.

The turbulent mean velocity profiles for concentrations below 21 ppm are plotted in Fig. 16. The profiles for the asymptotic cases are the solid circles and diamonds on Fig. 10 which are plotted with other polymer fluctuation flows. The asymptotic cases fit into an ordered sequence, as concentrations and strain rates are increased when viewed as laminar flows with polymer fluctuations. When viewed from the water turbulent limit, the mean velocity profiles increase their difference from the Newtonian turbulence as concentration increases, but then fall back as the asymptotic conditions are approached and polymer fluctuations play a dominant role.

The mean velocity profiles plotted in the standard wall coordinates are indicative of the effective viscosity in the different ranges in the flow. In the sublayer, $y^+ < 8$, the mean velocity profiles for laminar and turbulent water are the same and there is no evidence in our experiments that polymer flows with either polymer induced fluctuations or turbulence departs significantly from this solvent behavior. As far as the sublayer thickness is concerned, our results are in agreement with those of Reischman and Tiederman (ref. 8); however, the laminar water flow on the table departs from $U^+ = y^+$ in the neighborhood of $y^+ \approx 8$ (cf. Fig. 3) because the shear stress is not constant throughout the flow. The laminar water flow mean velocity profile represents what is expected when the viscosity is constant throughout the flow. On the other hand, the turbulent water flow profile is the result of augmentation of molecular viscosity by the turbulent mixing process. Departures from this profile for turbulent polymer flows imply changes in the mixing process. Following this line of reasoning, Fig. 16 shows a departure from the universal profile for 9 ppm at $u_\tau = 3.72$ cm/sec and the maximum departure at 14 ppm and $u_\tau = 3.77$ cm/sec. At this latter concentration, polymer fluctuations were observed at $u_\tau = 3.71$ cm/sec, which is near the boundary curve for Fig. 7. Increasing polymer concentration and strain rate appears to inhibit normal turbulent mixing; however, beyond the moderate concentration of 14 ppm fluctuations in the u-velocity are induced in the laminar flow resulting in an effective increased viscosity, at least in the region where the fluctuations are observed. The resulting turbulent flows at concentrations of 21 ppm and beyond appear not only to consist of suppressed turbulent mixing but also have augmented viscosity due to polymer fluctuations. Those turbulent flows with the lowest peak values of u'^+ appear to be dominated by polymer induced fluctuations observable at y^+ near the peak (Fig. 15) rather than by normal turbulent mixing processes which show a similar profile of u'^+ (cf. Fig. 5 for pure water of Fig. 12 for 9 ppm of polymer). Increasing the polymer concentration from 25 to 32 ppm increases the maximum of u'^+ relative to its value at 15 ppm and shifts the resulting mean turbulent velocity profile back toward the water turbulent curve. The shift is due to an increase in polymer fluctuations rather than due to increased turbulent mixing. The asymptotic flow situations exhibit more laminar features than turbulent ones. Spectra for this flow are shown in Fig. 15. The fluctuations are confined to the wall region, outside of which the velocity gives the appearance of a laminar flow with possibly presence of some very low frequencies.

Measurements of the average spanwise streak spacing, λ^+, were made of the polymer turbulent flows using the salt crystal technique. A few examples illustrate the results. For pure water $\lambda^+ = 116 \pm 15$; at concentration of 9 ppm and $u_\tau = 3.72$ cm/sec, $\lambda^+ = 161 \pm 115$; at 9 ppm and $u_\tau = 4.21$ cm/sec, $\lambda^+ = 200 \pm 18$; at 16 ppm and $u_\tau = 3.52$ cm/sec $\lambda^+ = 190 \pm 20$. For the flows at and near asymptotic conditions there was no evidence of streaks using this technique.

DISCUSSION OF RESULTS AND CONCLUSIONS

The flows investigated were two-dimensional laminar and turbulent shear flows on a free surface water table. These basic flows were characterized in detail. Measurements of U^+, u'^+ and u-velocity spectra versus y^+ have been reported along with observations of the free surface and measurements of spanwise streak spacing for turbulent flows. The laminar flow is nearly an equilibrium flow and in good agreement with the calculated profile assuming the body force is equal to the local wall shear stress. The turbulent flow mean velocity profile is in excellent agreement with the universal velocity profile even though the flow extends only to y^+ on the order of 100. The peak of u'^+ occurs at y^+ of 15 in agreement with the results of other investigations made in other turbulent boundary layers and in pipes, while the absence of the outer flows appears to just reduce the overall level of u'^+. The spanwise streak spacing is in agreement with published values of other investigators. The absence of the outer flow allowed the near wall region to be studied without the extraneous disturbances imposed by the outer flow. As a result, it has been possible to establish features of the inner flow which have not been revealed in other investigations.

At modest polymer concentrations and strain rates large enough to be comparable to the time scale of the polymer, effects on the velocity very near the wall become noticeable in an otherwise laminar flow. The mean intensity of polymer induced fluctuations has a spatial distribution in y^+ similar to what one finds in Newtonian turbulence, though the intensity is lower and spectral distribution is quite different.

The distinction is further confirmed by velocity time traces and the free surface appearance. No evidence of streaks in the flow were found at the wall. Transition to a polymer-influenced turbulence would be triggered by a large enough three-dimensional disturbance in the flow.

The polymer induced velocity fluctuations are clearly strain rate dependent as shown in Fig. 7. Since the strain rate where they are first observed is of the same order as the inverse of the calculated response time for the polymer, it is natural to assume these fluctuations are associated with at least partial expansion of the polymer. Observations of an increase in laminar wall shear stress in capillary flows at similar maximum strain rates have been ascribed to "early turbulence" (ref. 15). We have also observed an increase in wall shear stress when polymer induced fluctuations are present; however, this flow state is distinct from turbulence, since at modest polymer concentrations a separate and distinct transition can be induced. In addition, the spatial variation of u-velocity spectra shows that polymer induced fluctuations are primarily confined to the region near the wall with the fluctuations primarily in the 50 to 150 Hz range.

Turbulent flows of polymer solutions at low and modest concentrations or strain rates did exhibit streaks in the sublayer. The spacing between streaks increased with concentration and strain rate. In this regime, turbulent fluctuations were similar throughout the layer, and the spectra were similar to those of water. By comparing the depth of the polymer flow to that of water at the same mass flow rate and table inclination, drag reduction was definitely established. In addition, the mean velocity profiles showed a departure from the universal velocity profile, suggesting a change in turbulent mixing or effective turbulent viscosity. Polymer effects on the mean turbulent velocity profile and on wall shear stress were observed at polymer concentrations and strain rates below those needed to cause polymer fluctuations. Though no attempt was made to define an onset curve for polymer effects on turbulence similar to the one for polymer fluctuations in laminar flows, the experimental data suggest that the onset line lies to the left and below the polymer fluctuation curve of Fig. 7. Such a result is consistent with our view of hairpin eddies being the major mixing mechanism in a Newtonian turbulent boundary. The maximum strain rate in an eddy aligned with the flow would be higher than that at the wall, since the vortex tube forming the eddy is stretched by the mean flow. In addition, the maximum strain rate occurs where rotational effects are small, outside the vortex core. Hence, expansion of the polymer coil could occur at a lower strain rate than it could in the laminar shear flow at the wall where strain and rotation are in balance (ref. 2). For both of these reasons, it should be expected that polymers would begin to inhibit turbulent mixing at lower strain rates than in laminar flows. At a fixed concentration, strain rate dependence should also be expected. Polymers such as WSR-301 contain molecules of different lengths, and the largest expand at lower strain rates than the shorter molecules. Independent of the exact structure of the three-dimensional mixing mechanism, some of the structures will involve higher strain rate motions than others. It is these more intense structures which will be inhibited at the lowest strain rates, leading to an increase in turbulent streak spacing as strain rate is increased. Such reasoning is consistent with the experimental result presented. It is further confirmed by comparison of the u'^{+} spectrum across the flow as a function of concentration and strain rate. Fig. 5 is the water spectra and Fig. 12 is for 9 ppm, a concentration below polymer induced fluctuations; the spectra are quite similar, though drag reduction is observed and the mean velocity profile has been influenced indicating a change in mixing. Increasing concentration and strain rate, Figs. 13 and 14 show the velocity fluctuations substantially reduced except for $y^{+} < 20$, where polymer induced fluctuations are found in laminar flows. With further increase in strain rate and concentration, an asymptotic regime is reached where most of the turbulent features are suppressed but the polymer induced velocity fluctuations remain (Fig. 15). Under these conditions, streaks were never observed. These suppressed turbulent flows have mostly laminar characteristics, and it was difficult to distinguish these flows from those of polymer induced fluctuations at similar strain rates and concentrations.

On the basis of the flows so far investigated, it is possible to speculate on what would happen if concentration and strain rate were both substantially increased. It is believed that the flow would remain suppressed but the level of u'^{+} would increase. If this should be the case, then perhaps the very substantial difference between the u'^{+}

maxima measured by Reischman and Tiederman (ref. 8) and those measured by Rudd (ref. 5) could be explained.

Of the other investigations which obtained extensive velocity measurements (using LDA) in the near wall region of a turbulent drag reducing flow, Reischman and Tiederman (ref. 8) operated at essentially the same range of strain rates as we did, Kumor and Sylvestor (ref. 7) were very slightly higher, and Rudd (ref. 5) was nearly an order of magnitude higher ($\sim 10^4$ sec^{-1}). (Logan [ref. 6] did not report strain or u_τ.) All of these investigators used 100 ppm or more of a similar or longer more effective drag reducing polymer than WSR-301. Thus, we expect that each of these investigations measured flows for which the near wall layers could be characterized as suppressed turbulence and that the u'^+ measurements reported were composed mainly of polymer induced fluctuations and fluctuations imposed by the outer flow which were not involved in mixing near the wall. Since the water table experiments reported here extended only to y^+ of 100, direct comparison is difficult and somewhat conjectural. Closed comparisons would have been possible if velocity spectral data had been measured by the other investigators.

The selective seeding of the flow with hydrogen bubbles, which allowed detailed spatial resolution and spectral measurement of the velocity to be made, is believed to be novel. Its use in conjunction with visual observations of the free surface disturbances enabled the laminar-like polymer induced velocity fluctuation flow to be identified.

Comparisons with other research have been made on the basis of wall strain rates. If one were to determine Reynolds numbers appropriate for water table flows, using thickness as the length parameter, they would certainly be much lower than the Reynolds numbers of previous investigations (Refs. 5-9), yet the very suitability of drawing conclusions from a Reynolds number comparison is questionable due to the inherent differences of the water table flow from those in pipes or over a flat plate. Since it is fairly well established that drag reduction due to polymer additives is a wall phenomenon, using wall variables appears to be the most reasonable approach for comparison.

ACKNOWLEDGEMENTS

It is with pleasure and gratitude that we acknowledge the financial support of the Division of Engineering and Applied Physics, Harvard University, Cambridge, Mass. and the U.S.A. Office of Naval Research and the Fluid Mechanics Program of the USA National Science Foundation Grant #NSF-ENG77-01478

REFERENCES

1. Lumley, J. L. "Drag reduction by additives" Ann. Rev. Fluid Mech., 1, pp.367 ff. (1969)

2. Lumley, J. L. "Drag reduction in turbulent flow by polymer additives" J. Polymer Sci. Macromolecular Reviews 7, pp. 263-290 (1973)

3. Hoyt, J. W. "The effect of additives on fluid friction" J. Basic Engg. D94, pp. 258-285 (1972)

4. Virk, P. S. "Turbulent kinetic energy profile during drag reduction" Phys. Fluid, 18, pp. 415 ff. (1975)

5. Rudd, M. J. "Velocity measurements made with a laser Dopplermeter on the turbulent pipe flow of a dilute polymer solution" J. Fluid Mech. 51, pp. 673-685 (1972)

6. Logan, S. E. "Laser velocimeter measurement of Reynolds stress and turbulence in dilute polymer solutions" Am. Inst. Aeronautics and Astronautics J. 10, pp. 962 ff. (1972)

7. Kumor,S. M. & Sylvestor, N. D. "Effects of a drag-reducing polymer on the turbulent boundary layer" AIChE Symposium Series, Drag Reduction, pp. 1 ff.(1973)

8. Reischman, M. M. & Tiederman, W. G. "Laser-Doppler anemometer measurements in drag-reducing channel flows" J. Fluid Mech. 70, pp. 369 ff. (1975)

9. Scrivener, O. "A contribution on modifications of velocity profiles and turbulence structure in a drag reducing solution" Proc. Int. Conf. on Drag Reduction, BHRA Fluid Engg. pp. C66 ff.(1974)

10. Schraub, F. A., Kline, S. J. Henry, J. Runstadler, P. W. Jr., Littell, A. "Use of hydrogen bubbles for quantitative determination of time-dependent velocity fields in low-speed water flows" J. Basic Engg. ASME Trans. Series D87, pp. 429 ff.(1965)

11. Gordon, R. J. & Balakrishnan, C. "Vortex inhibition: a new viscoelastic effect with importance in drag reduction and polymer characterization" J. Appl. Pol. Sci. 16, pp. 1629 ff. (1972)

12. Hinze, J. O. "Turbulence" 2nd edition, McGraw Hill, pp. 627-628, 657 (1975)

13. Emmons, H. W. "The laminar-turbulent transition in a boundary layer" Part I. J. Aero Sci. 18, pp. 490-498 (1951)

14. Wygnanski, I. Sokolov, M. & Friedman, D. "On a turbulent 'spot' in a laminar boundary layer" J. Fluid Mech. 78, pp. 785 ff. (1976)

15. Forame, P. C., Hansen,R. J. & Little, R. C. "Observations of early turbulence in the pipe flow of drag reducing polymer solutions",AIChE J. 18, pp. 213 ff. (1972)

16. Berman, N. S. & George, W. K. "Onset of drag reduction in dilute polymer solutions" Phys. of Fluids, 17, pp. 250-251(1974)

17. Paterson, R. W. & Abernathy, F. H. "Turbulent flow drag reduction and degradation with dilute polymer solutions" J. Fluid Mech. 43, pp. 689-710 (1970)

18. Hansen, R. J., Little, R. C., Reischman, M. M. & Kelleher, M. D. "Stability and the laminar-to-turbulent transition in the pipe flows of drag-reducing polymer solutions", BHRA, Int. Conf. on Drag Reduction (1974)

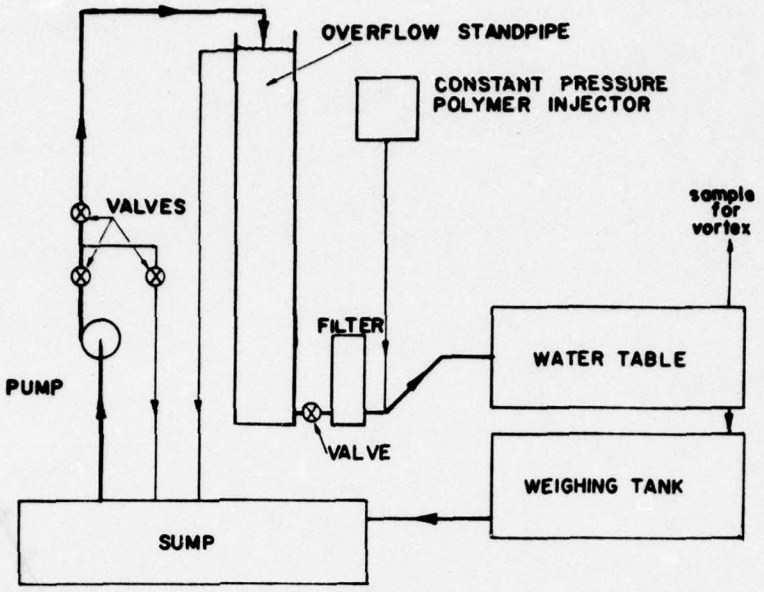

Fig. 1 Schematic flow arrangement

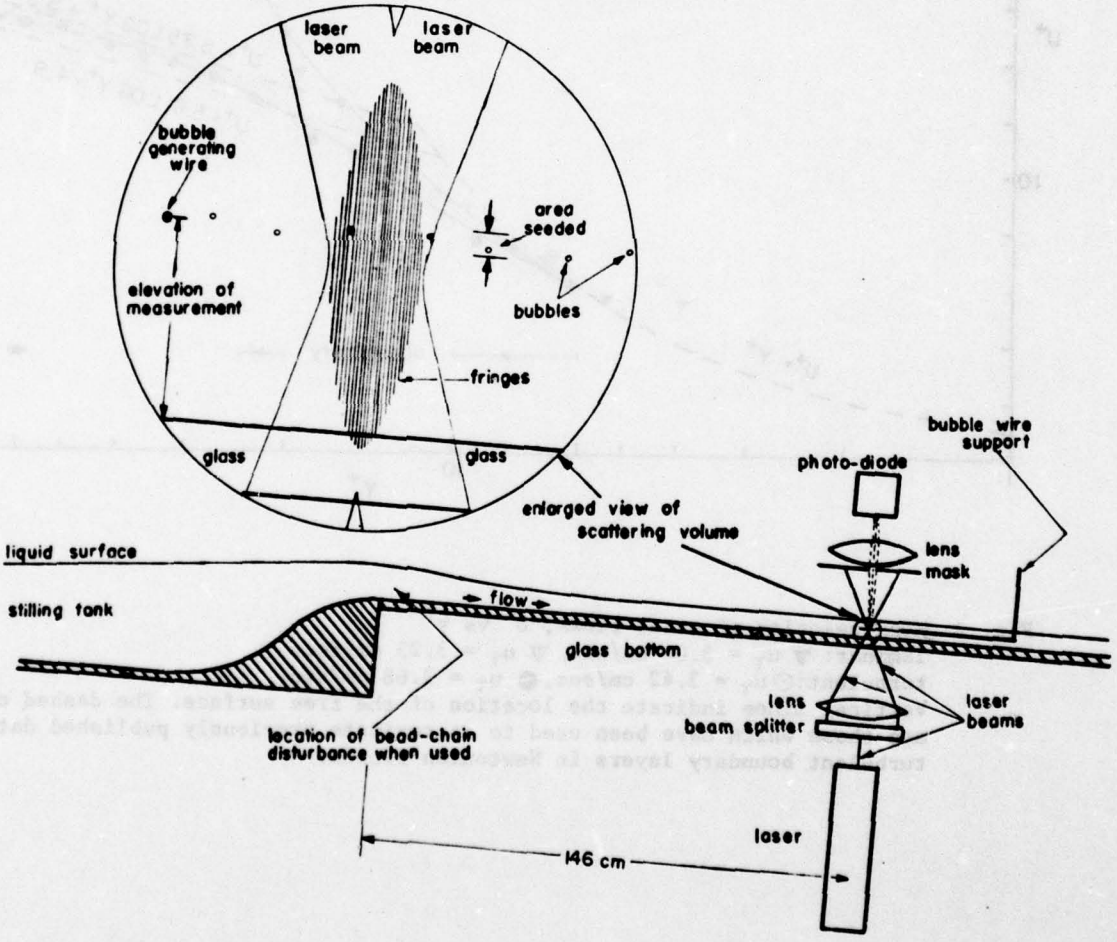

Fig. 2 Side view of water table showing the orientation of the laser-Doppler anemometer. The detailed view depicts the selective seeding method in which bubbles generated by electrolysis and introduced at a narrow range of y are used with the LDA.

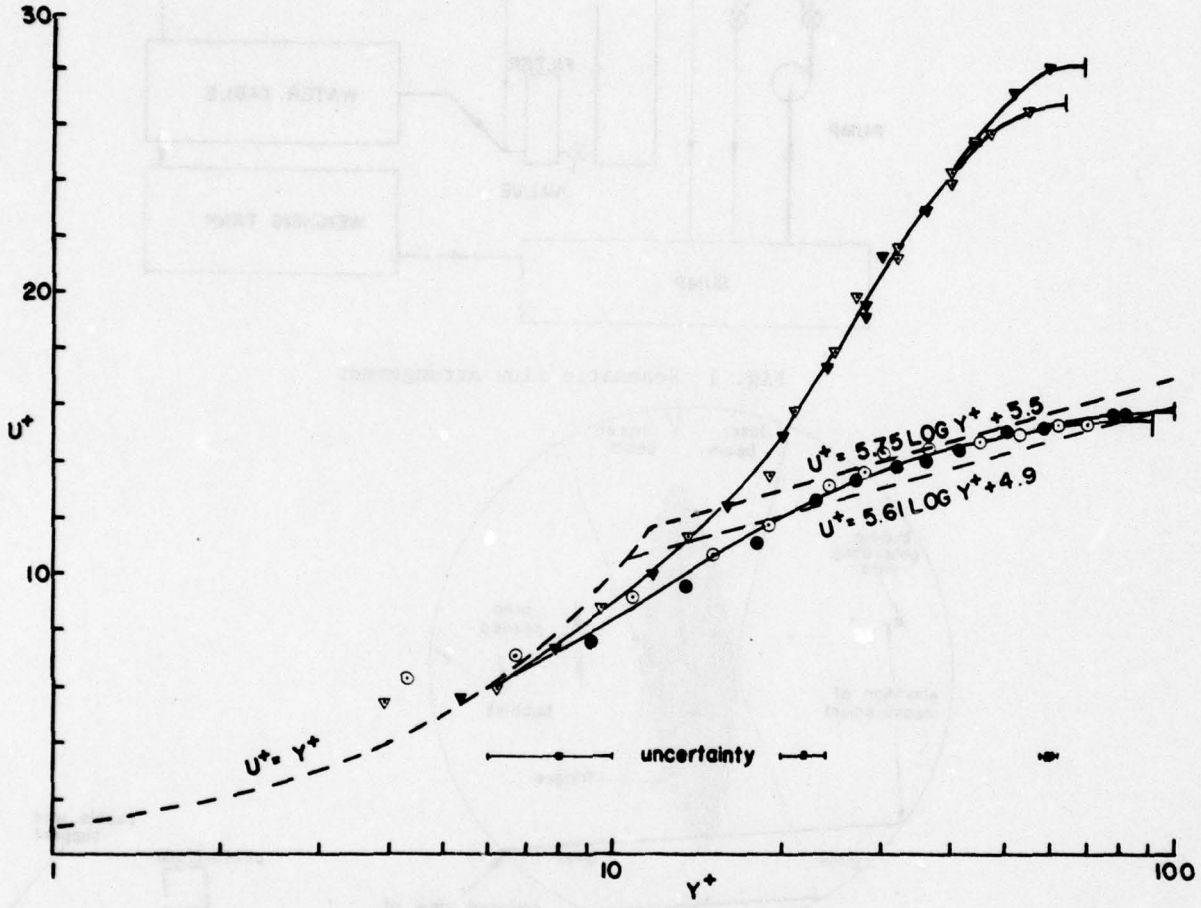

Fig. 3 Mean velocity of water flows, U^+ vs y^+
laminar: ▼ u_τ = 3.04 cm/sec, ▽ u_τ = 3.25 cm/sec;
turbulent: ⊙ u_τ = 3.42 cm/sec, ● u_τ = 3.68 cm/sec.
Vertical lines indicate the location of the free surface. The dashed curves are those which have been used to approximate previously published data for turbulent boundary layers in Newtonian fluids.

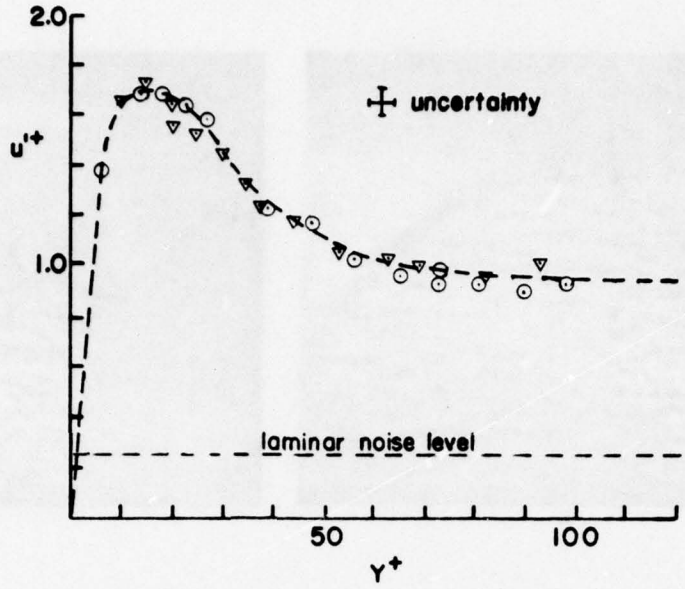

Fig. 4 Turbulent water u'^+ vs y^+. All u'^+ data has been corrected for the laminar LDA noise whose uncorrected level is shown.
⊙ u_τ = 3.42 cm/sec. ▽ u_τ = 3.83 cm/sec.

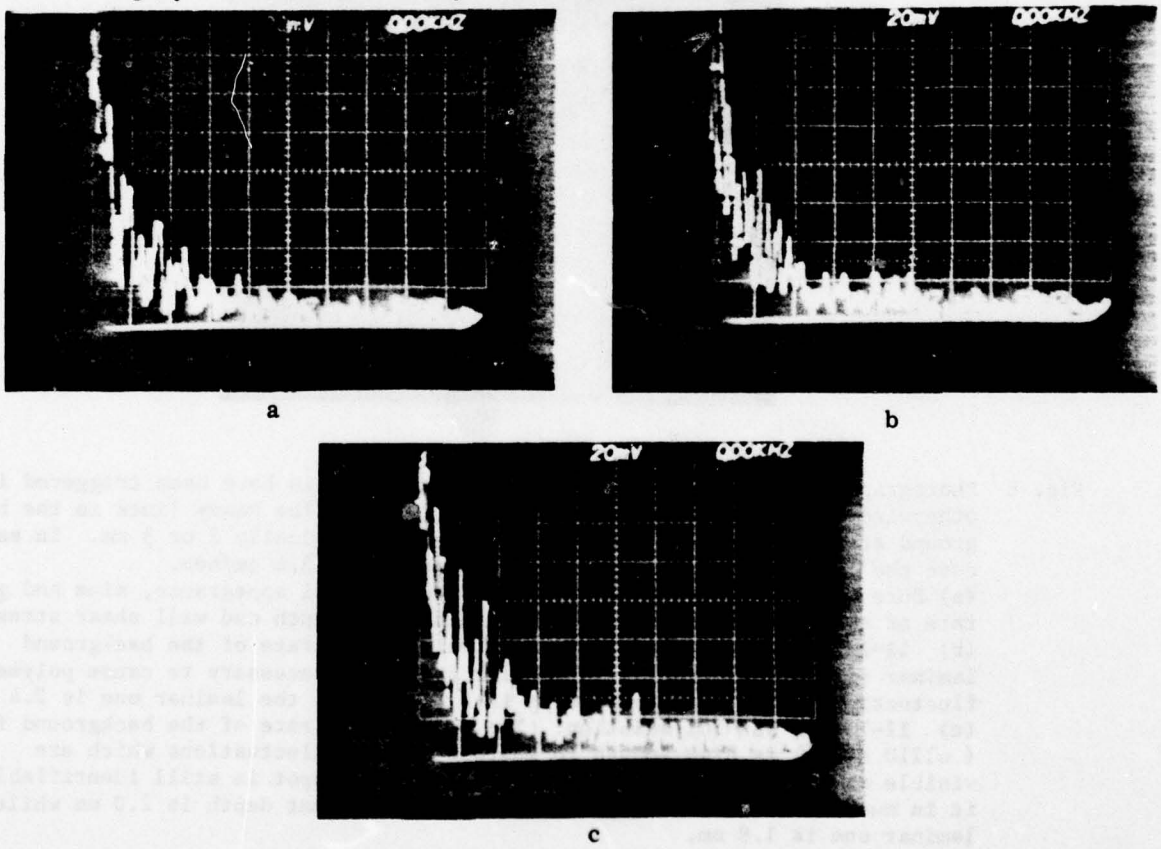

a b c

Fig. 5 Water turbulence spectra: as for all spectral data presented (Figs. 9, 12-15) full scale is 500 Hz and the vertical amplitude is 20 mV rms per division. u_τ = 3.71 cm/sec. (a) y^+ = 58 (b) y^+ = 48 (c) y^+ = 14. The water turbulence spectra are essentially similar to these over the range of u_τ and y^+ investigated.

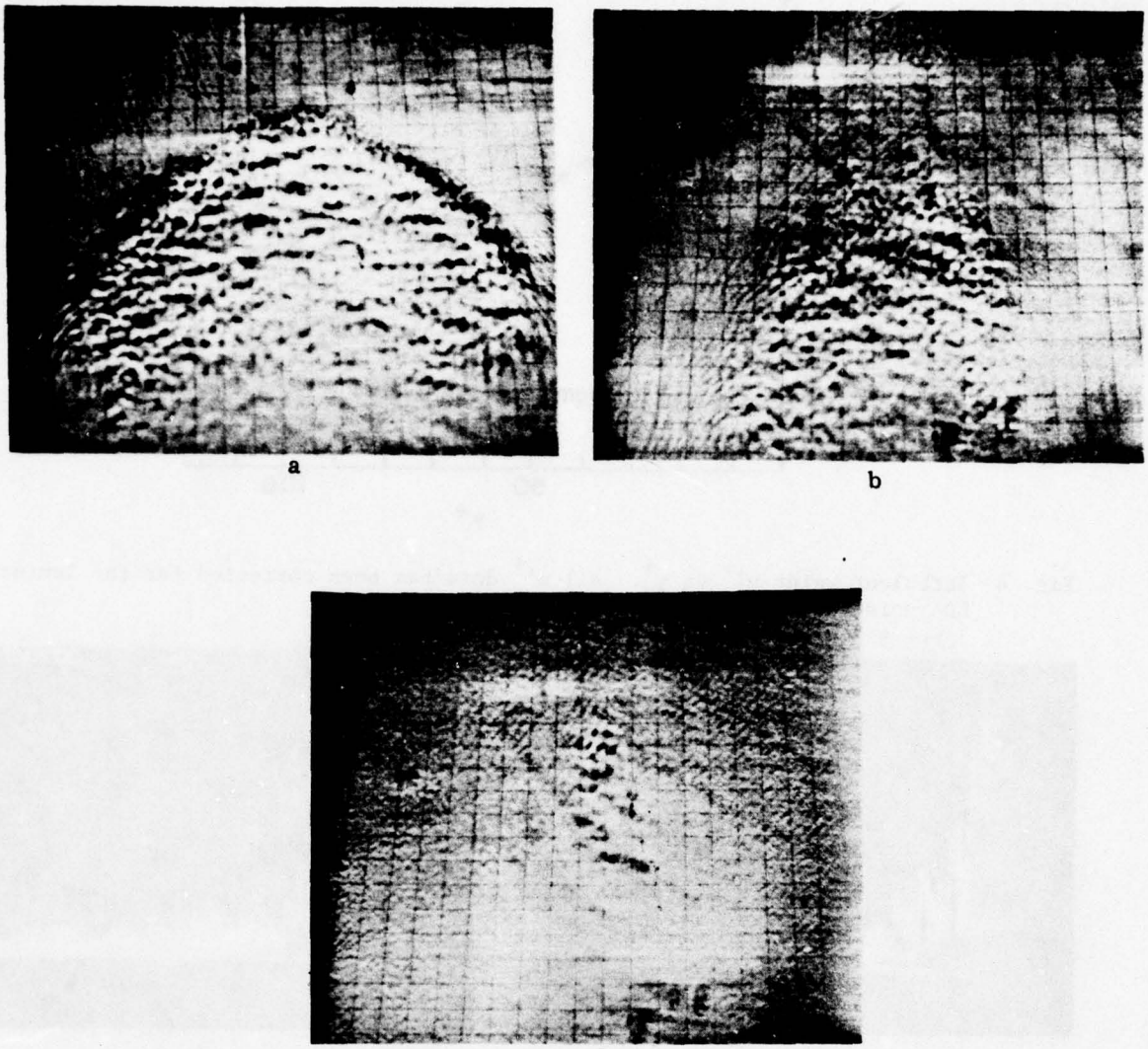

Fig. 6 Photographs of the free surface when turbulent spots have been triggered in an otherwise undisturbed flow over the water table. The heavy lines in the background are 2.54 cm apart and the flow depth is typically 2 or 3 mm. In each case the fully turbulent depth corresponds to $u_T \simeq 3.6$ cm/sec.
(a) Pure water. Over the range studied the general appearance, size and growth rate of the spot are essentially independent of depth and wall shear stress.
(b) 11-13 ppm WSR-301 solution. The wall strain rate of the background laminar flow ($\simeq$1130 sec^{-1}) is smaller than that necessary to cause polymer fluctuations. The turbulent depth is 2.8 mm while the laminar one is 2.4 mm.
(c) 11-13 ppm WSR-301 solution. The wall strain rate of the background flow ($\simeq$1210 sec^{-1}) is high enough to sustain polymer fluctuations which are visible as ripples on the free surface. While a spot is still identifiable, it is much less distinct than in (b). The turbulent depth is 2.0 mm while the laminar one is 1.9 mm.

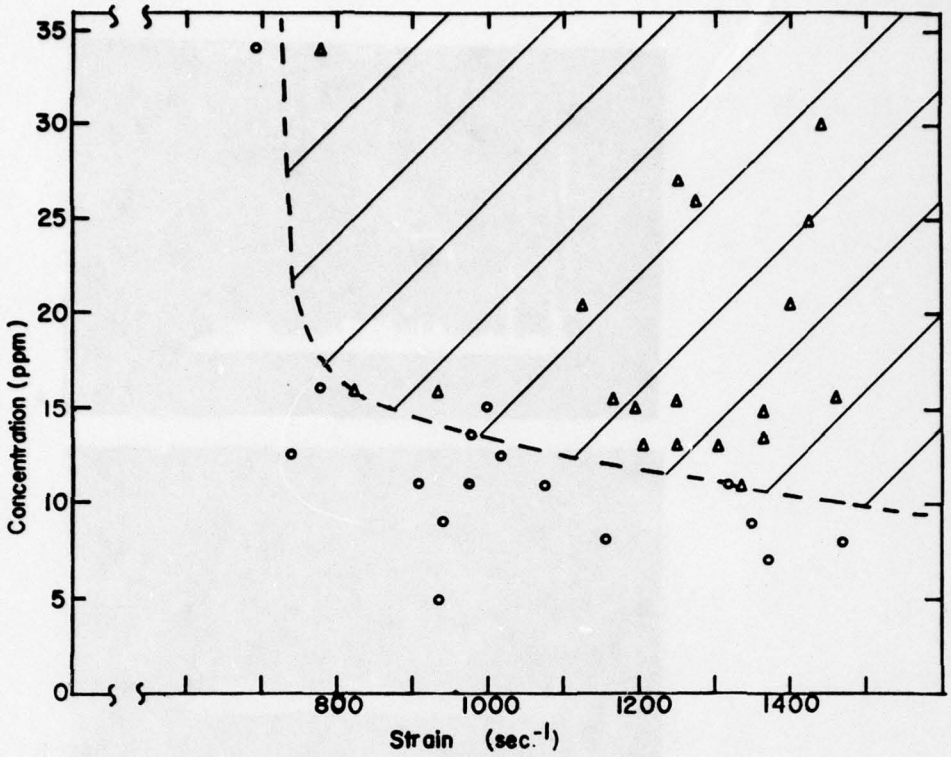

Fig. 7 Observations of polymer solution flows without disturbance as a function of concentration and strain rate (dU/dy). ○ smooth free surface: ▽ rippled free surface indicating the presence of polymer fluctuations (cf. the background of Fig. 6c). Fluctuations are expected in the shaded region.

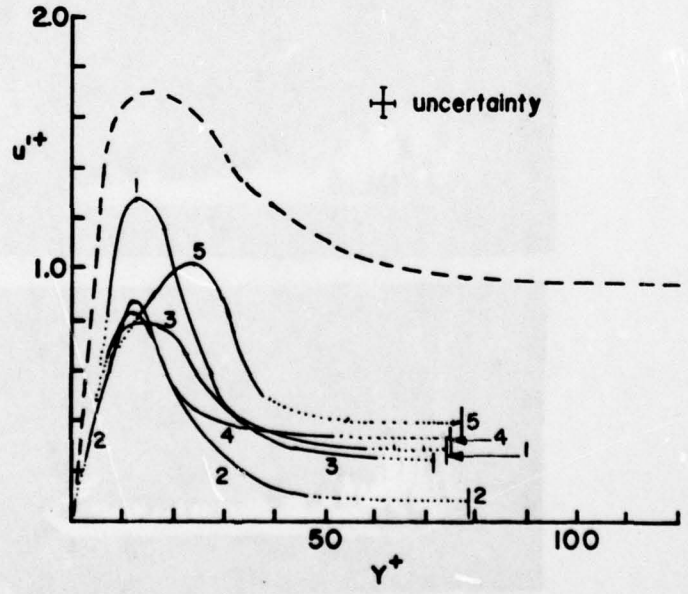

Fig. 8 Polymer induced fluctuations, u'^{+} vs y^{+} (in rough order of increasing activity). (1) 14 ppm, u_τ = 3.71 cm/sec. (2) 16 ppm, u_τ = 3.36 cm/sec. (3) 15 ppm, u_τ = 3.65 cm/sec. (4) 25 ppm, u_τ = 3.73 cm/sec. (5) 32 ppm, u_τ = 3.81 cm/sec. The dashed curve is u'^{+} vs y^{+} for turbulent water. A vertical line indicates the location of the free surface. Dotted lines indicate extrapolation beyond data points.

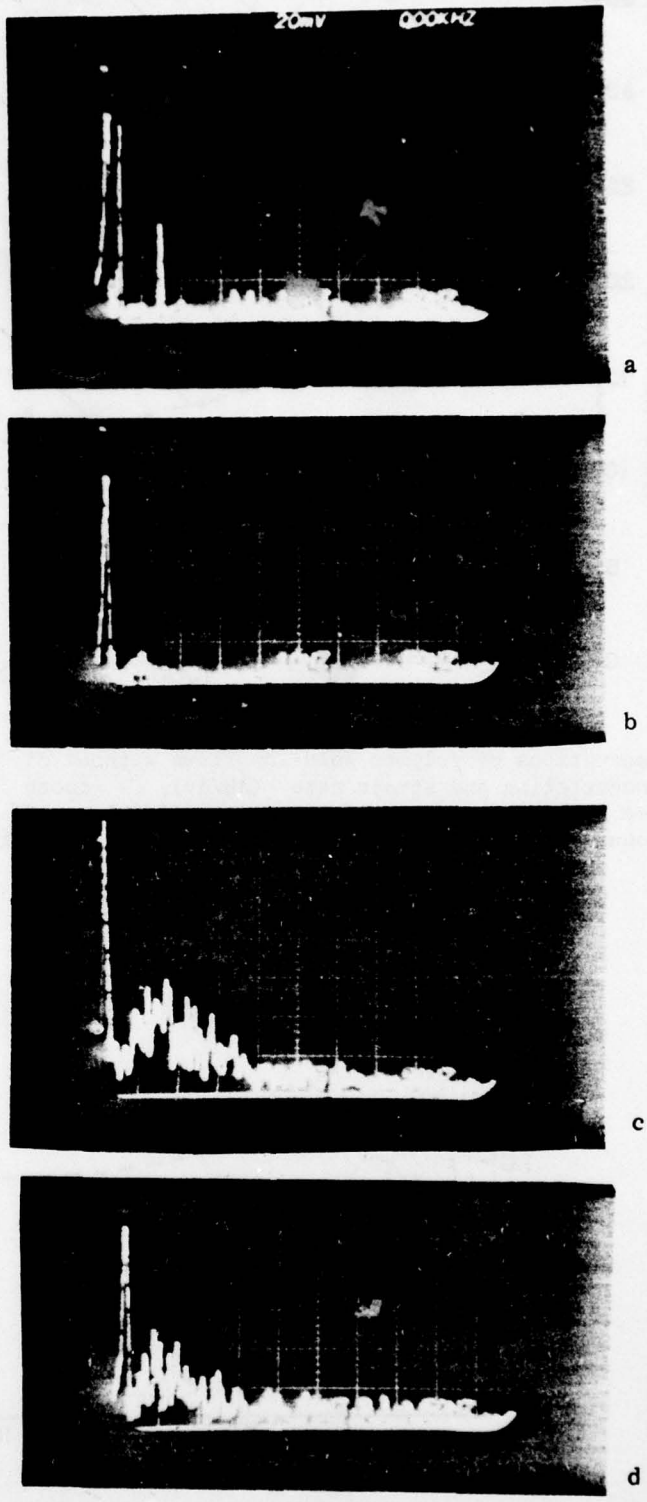

Fig. 9 Polymer fluctuation spectra: 16 ppm, u_τ = 3.36 cm/sec.
(a) y^+ = 57 (b) y^+ = 39 (c) y^+ = 12 (d) y^+ = 8
The enriched spectral amplitude at 50-150 Hz is clearly visible near the wall.
This is the same flow as curve 2 in Fig. 8

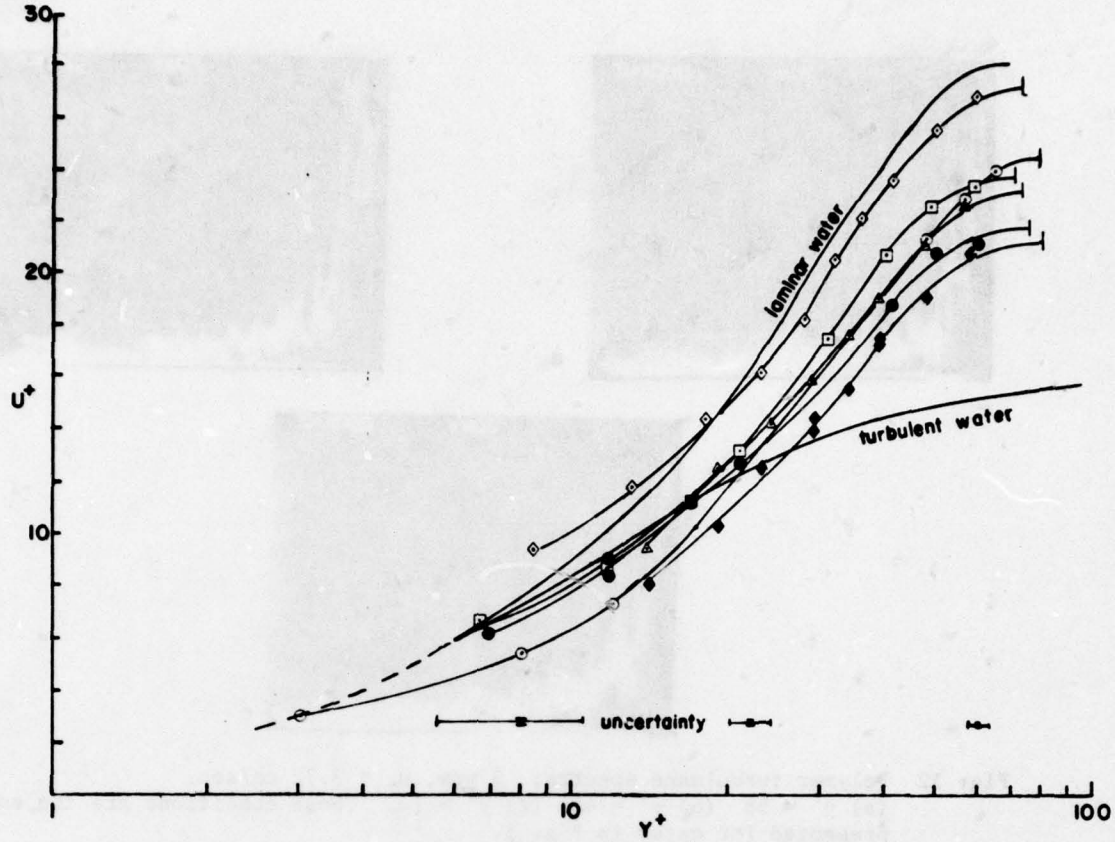

Fig. 10 Polymer induced fluctuation flows, U^+ vs y^+, roughly in order of increasing polymer activity.

◇ 14 ppm, u_τ = 3.71 cm/sec. △ 21 ppm, u_τ = 3.72 cm/sec.
⊡ 15 ppm, u_τ = 3.65 cm/sec. ● 25 ppm, u_τ = 3.73 cm/sec.
⊙ 16 ppm, u_τ = 3.36 cm/sec. ◆ 32 ppm, u_τ = 3.85 cm/sec.

These last two cases are at the asymptotic limit and the mean velocity profiles are practically identical to those of suppressed turbulence at the same u_τ and concentration.

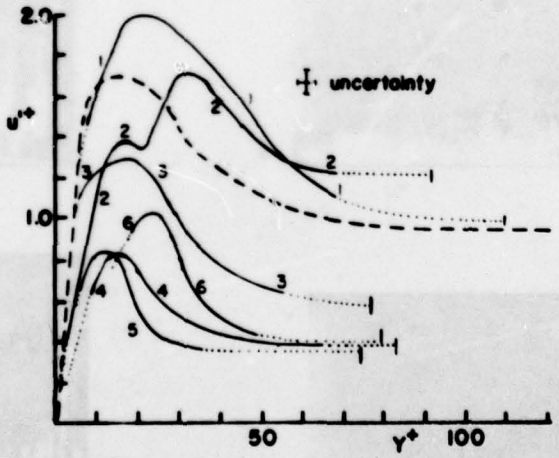

Fig. 11 Polymer turbulence u'^+ vs y^+

(1) 9 ppm, u_τ = 3.72 cm/sec. (2) 16 ppm, u_τ = 3.52 cm/sec.
(3) 15 ppm, u_τ = 3.25 cm/sec. (4) 16 ppm, u_τ = 3.85 cm/sec.
(5) 25 ppm, u_τ = 3.73 cm/sec. (6) 32 ppm, u_τ = 3.85 cm/sec.

A vertical line indicates the location of the free surface, and dotted lines are extrapolations beyond data points.

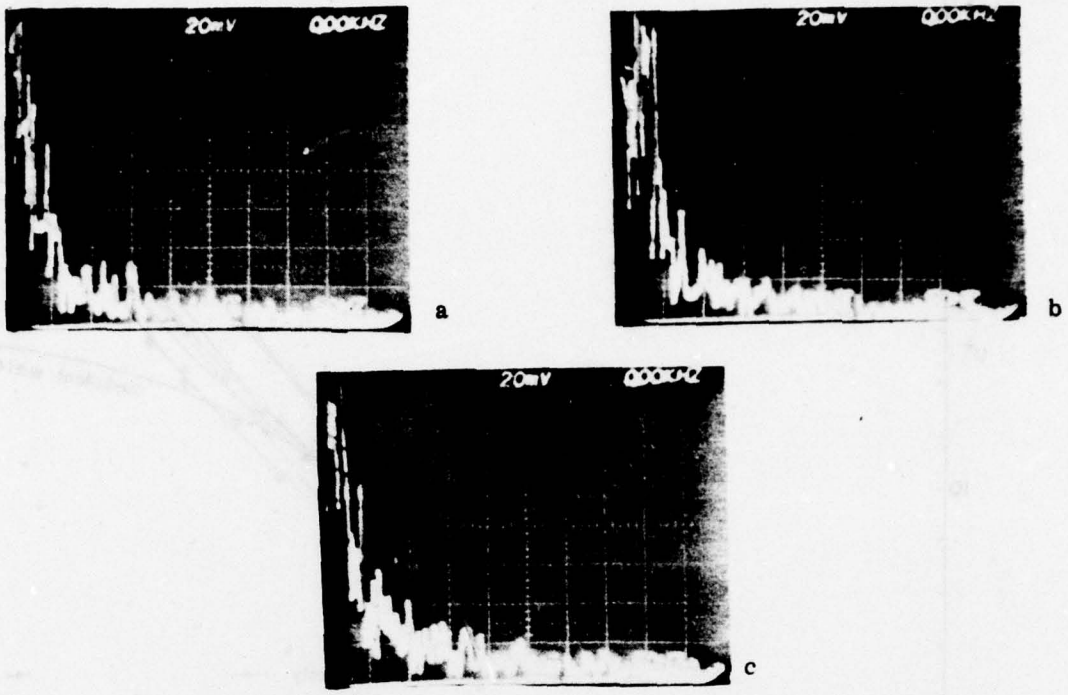

a b c

Fig. 12 Polymer turbulence spectra; 9 ppm, u_τ = 3.72 cm/sec.
(a) y^+ = 58 (b) y^+ = 48 (c) y^+ = 14. These conditions are the same as presented for water in Fig. 5.

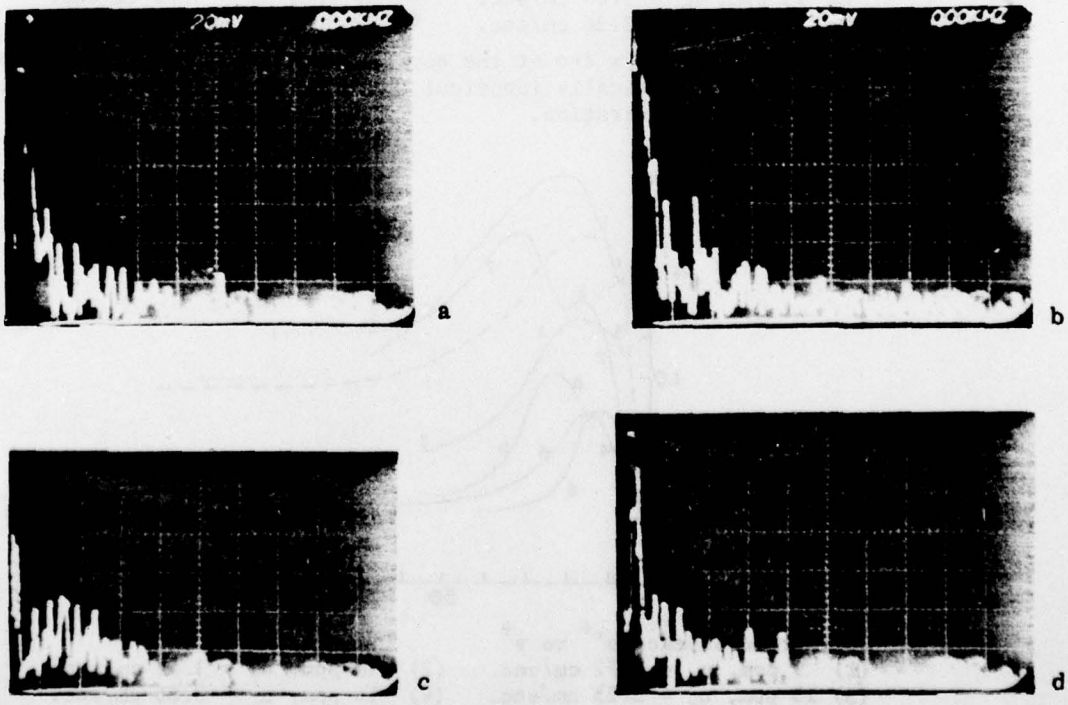

a b c d

Fig. 13 Polymer turbulence spectra: 16 ppm, u_τ = 3.52 cm/sec.
(a) y^+ = 41 (b) y^+ = 32 (c) y^+ = 13 (d) y^+ = 8
This is the same flow as for curve 2 of Fig. 11. Note that at y^+ = 13, the spectrum is similar to those for polymer fluctuations. (Fig. 9).

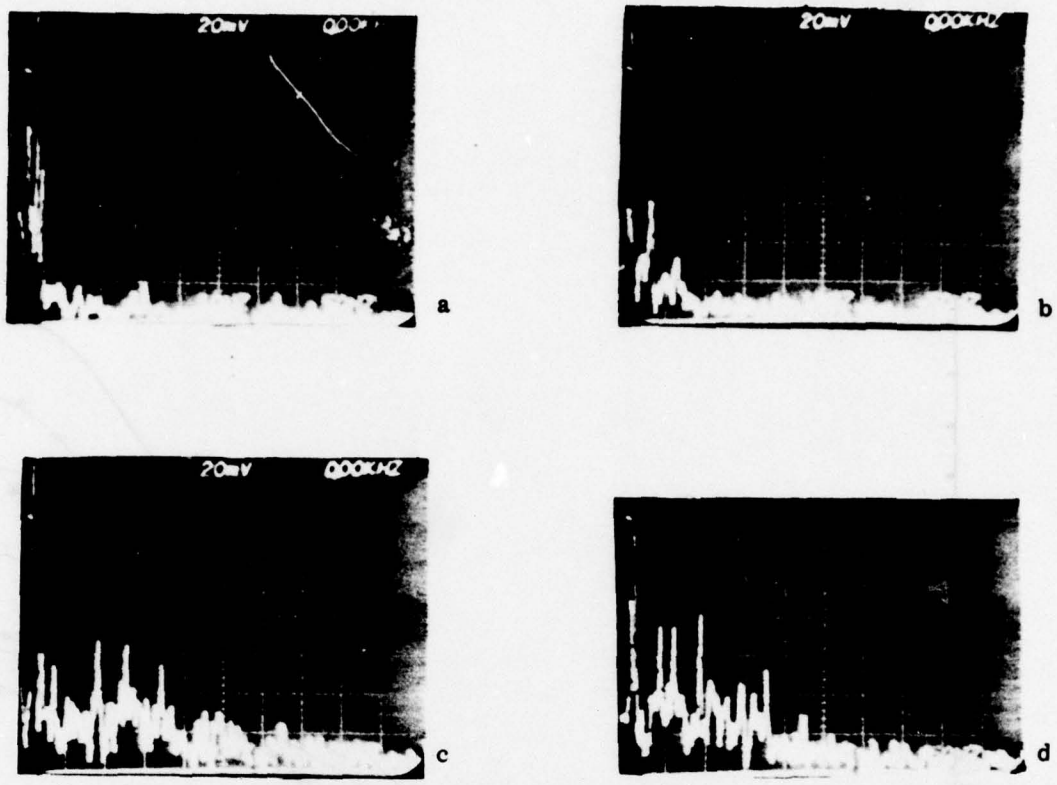

Fig. 14 Polymer turbulence spectra: 16 ppm, u_τ = 3.85 cm/sec. (a) y^+ = 54 (b) y^+ = 35 (c) y^+ = 19 (d) y^+ = 14. This is the same flow as for curve 4 of Fig. 11.

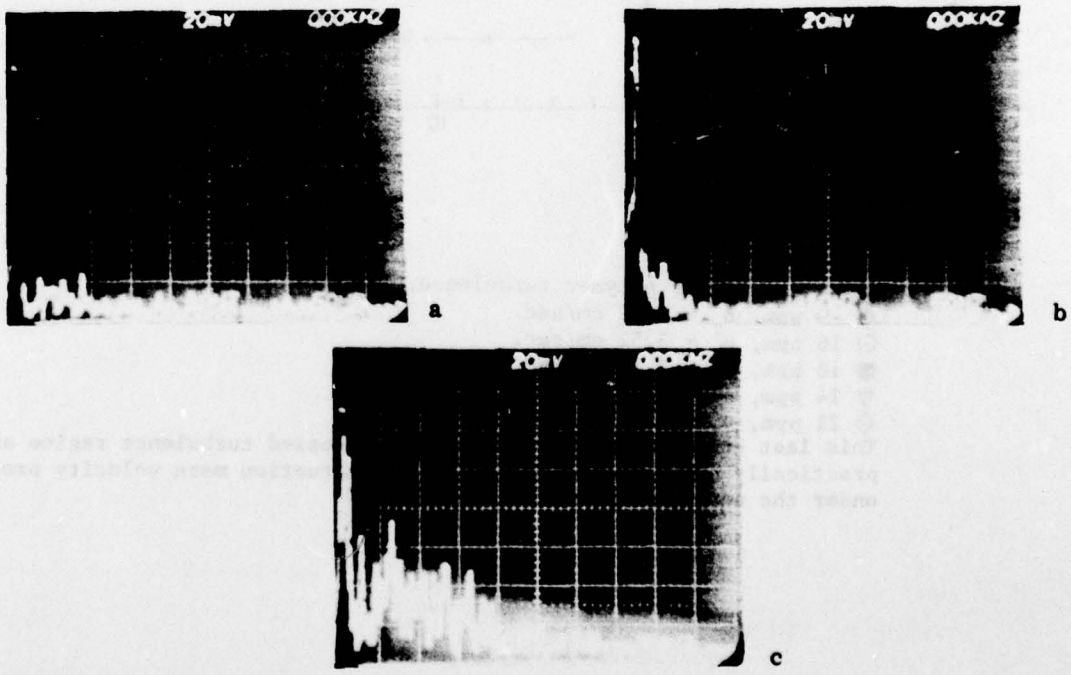

Fig. 15 Polymer turbulence spectra: 25 ppm, u_τ = 3.73 cm/sec. (suppressed turbulent regime) (a) y^+ = 50 (b) y^+ = 26 (c) y^+ = 12. This is the same flow as curve 5 of Fig. 11. The laminar counterpart of this flow had essentially identical spectra.

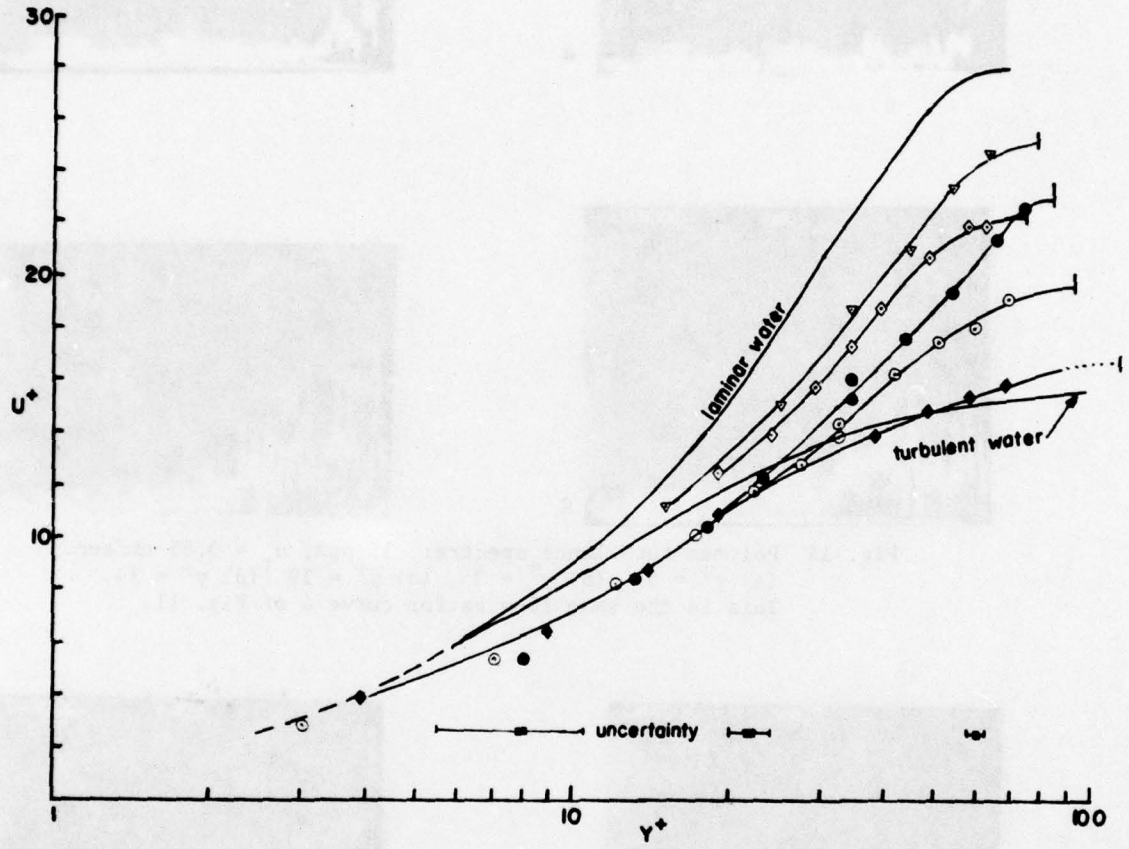

Fig. 16 Mean velocity of polymer turbulence, U^+ vs y^+

◆ 9 ppm, u_τ = 3.72 cm/sec.
⊙ 16 ppm, u_τ = 3.52 cm/sec.
● 16 ppm, u_τ = 3.85 cm/sec.
▽ 14 ppm, u_τ = 3.77 cm/sec.
◇ 21 ppm, u_τ = 3.73 cm/sec.

This last case is an example of the suppressed turbulence regime and is practically identical to the polymer fluctuation mean velocity profile under the same conditions.

APPENDIX I - b

TURBULENCE SPECTRA USING LASER-DOPPLER ANEMOMETRY AND SELECTIVE SEEDING

Frederick H. Abernathy, John R. Bertschy,
& Robert W. Chin
Division of Applied Sciences, Pierce Hall
Harvard University, Cambridge, Mass. 02138

Presented at the Biennial
Turbulence Conference at
the Univ. of Missouri-Rolla
Oct. 3-5, 1977.

ABSTRACT

A novel method of improving the spatial resolution of a laser-Doppler anemometer in water flows has been developed. Bubbles generated by electrolysis from a small diameter platinum alloy wire located upstream of the laser scattering volume is used to scatter light for the anemometer. Most of the indigenous scattering particles are filtered from the flow. The bubble generation can be large enough to obtain a nearly continuous velocity signal from the laser anemometer, allowing spectra and other detailed velocity measurements to be obtained. Results are presented comparing hot-film measurements with those obtained using the selective seeding method. Comparisons are presented for a turbulent flow in a flume and for laminar and turbulent boundary layer flows involving very steep velocity gradients.

NOMENCLATURE

C_D	drag coefficient of circular cylinder
d	diameter of bubble wire 25μ
R(22)	ratio voltage response of the LDA using 22mm beam separation to that of the hot film probe
R(50)	ratio voltage response of the LDA using 50mm beam separation to that of the hot film probe
$Re = \frac{U_{\infty} d}{\nu}$	Reynolds number based on free stream velocity and wire diameter
U	local mean velocity on the water table
U_{∞}	free stream velocity
u	local bubble velocity
u_{τ}	wall friction velocity
x	distance from bubble wire to scattering volume in the stream direction
y	distance normal to the wire wake or distance away from the wall
$y^+ = \frac{y u_{\tau}}{\nu}$	non-dimensional distance from the wall
ν	kinematic viscosity

INTRODUCTION

In order to investigate the effects of strain rates on dilute polymer solutions, it was necessary to obtain velocity measurements within boundary layers typically 2mm thick (Bertschy & Abernathy, 1977). A laser-Doppler anemometer (LDA) was chosen to obtain true velocity measurements of these non-Newtonian flows; however, spatial resolution remained a problem. The scattering volume formed by the intersecting laser beams of an LDA operated in the dual beam mode depends on the specific geometry of the optical system and is typically on the order of 0.11mm dia. and 1.6mm in length. If the long axis of the scattering volume was aligned spanwise to the flow, some spatial resolution was possible but a sophisticated optical support would have been necessary to traverse the LDA system to obtain a flow profile. If the long axis was aligned normally to the surface, across the velocity gradient, then spatial resolution was impossible. Consequently for shear layers of the dimensions described, it was difficult if not impossible to distinguish the signal of a laminar flow from one of turbulent flow. To overcome this limitation in spatial resolution of an LDA system, a selective seeding technique was developed which works well with water flows.

The essence of the technique is to filter out most of the scattering particles from the water, and then introduce a thin sheet of hydrogen or oxygen bubbles upstream of the scattering volume, and perpendicular to its long axis. The intersection of the sheet of bubbles and the LDA optical volume then constitutes the effective scattering volume, thereby reducing its effective length. With sufficient bubble density, a nearly continuous velocity measurement can be obtained which is essential for some measurements.

The emphasis of this paper is to establish the basis for using the selective seeding technique and comparing its results with those obtained from standard instrumentation. To this end, measurements taken in an

open channel flow with an LDA system using standard natural seeding and with a hot-film sensor were compared to measurements obtained using selective seeding. To establish the validity of the selective seeding technique in a flow with steep velocity gradients, its results were compared with those obtained from a hot film sensor in a flow over a water table.

BUBBLE VELOCITY

Hydrogen bubbles generated by electrolysis in water have been used for generating fluid flow markers; most of the films produced under the direction of the National Committee for Fluid Mechanics Films (Shapiro (1972)) used the bubble technique for flow visualization. Schraub et. al. (1965) were early developers of the technique and reported data suggesting that the generating wire wake had negligible effects on bubble velocity at a distance, x, greater than 70 wire diameters. More recent measurements by Grass (1971) suggest that even at 750 wire diameters the wire wake causes the bubbles to move measurably more slowly than the flow outside of the wake. Since each of these observations was derived from high speed motion pictures and consequently had substantial uncertainty in velocity, we undertook an independent measurement of bubble velocity in the generating wire wake. The measurements were made in free surface water flume, 60 channel widths from the entrance where flow conditions are independent of distance along the channel, or in the discharge of a 2.54cm nozzle. The results are shown in figure 1, along with those of Grass (1971) and the calculated centerline velocity of a laminar wake. The velocity of the bubbles u, and the free stream velocity U_o were both obtained from LDA measurements. The free stream velocity was measured without a bubble wire in place, using the ambient particles in the water as light scatterers. The results are for four different Reynolds numbers spanning the range of free stream velocities generally encountered in free surface flows. In all cases, the wire diameter, d, was 25μ. There does not appear to be any Reynolds number dependence for the velocity defect, which at first seemed surprising. The dashed line called the laminar wake is a reasonable fit to the bubble velocity data for $300 < x/d < 1000$, a convenient distance range for the selective seeding technique. The laminar wake curve is the theoretical center line velocity defect for the laminar wake behind a two dimensional object with no consideration of bubble generation. The theoretical form of such a

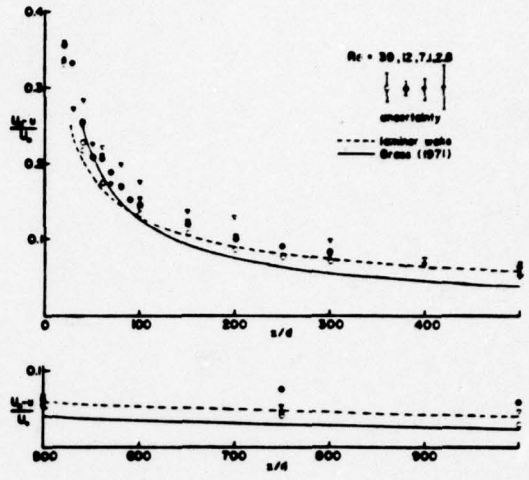

FIGURE 1: BUBBLE VELOCITY DEFECT $\frac{U_o - u}{U_o}$ vs x/d. THE UNCERTAINTY SHOWN IS ASSOCIATED SOLELY WITH ELECTRONICS.

○ Re = 39 ▼ Re = 7.1

● Re = 12 ▽ Re = 2.8

------LAMINAR WAKE CENTERLINE DEFECT (EQU. 3)

———GRASS (1971)

wake far downstream is

$$\frac{U_o - u}{U_o} = \frac{C_D\sqrt{Re}}{4\sqrt{\pi}} \left(\frac{x}{d}\right)^{1/2} e^{-\frac{y^2 U_o}{4\nu x}} \qquad (1)$$

and is given in many references (e.g. Schlichting, 1968). The Reynolds number dependence appears explicitly in the square root term and implicitly in the drag coefficient, C_D. A plot of $\frac{C_D\sqrt{Re}}{4\sqrt{\pi}}$ versus Reynolds number is shown in figure 2 where the values of C_D as a function of Re are from Tritton's (1959) experimental measurements using cylindrical rods.

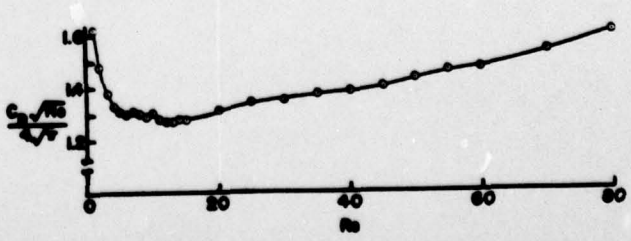

FIGURE 2. THE NUMERICAL COEFFICIENT OF THE LAMINAR WAKE SOLUTION (EQU. 1) FOR A CIRCULAR CYLINDER, $C_D\sqrt{Re}/4\sqrt{\pi}$, vs Re. C_D WAS DETERMINED USING TRITTON'S (1959) DATA.

When $3 < Re < 40$, the product $\frac{C_D\sqrt{Re}}{4\sqrt{\pi}}$ only varies from 1.26 to 1.38. We have taken this product to be a constant 1.30 yielding the following equation for the centerline velocity defect

$$\frac{U_o - u}{U_o} = 1.30\left(\frac{x}{d}\right)^{-1/2} \qquad (2)$$

This is shown as a dashed curve in figure 1 which is a reasonable fit to the measured data for $2.8 < Re < 39$. The solid curve of figure 1,

$$\frac{U_o - u}{U_o} = 3.62\left(\frac{x}{d}\right)^{-0.729} \qquad (3)$$

due to Grass (1971) represents a best fit to his motion picture data. The uncertainty in his measurements of the flow Reynolds number was not given. The uncertainty displayed in figure 1 is merely associated with the difference between two velocities of nearly equal size, each known to $\pm$ 1%. Greater effort was not spent in reducing the uncertainty since the correction itself is small, for example $6.5 \pm 2\%$ at $x/d = 400$.

The conclusion to be drawn from figures 1 and 2 is that hydrogen bubbles generated by a wire in the flow do follow the fluid flow, bearing in mind that correction is necessary for the wire wake. The correction is adequately described by equ. 2 for the range $3 < Re < 40$.

VELOCITY MEASUREMENTS

The velocity measurements of figure 1 were presented without much information about the velocity signals themselves. Two somewhat different techniques were used. Without the introduction of hydrogen bubbles, one must rely on the uniformly distributed solid particles in the water to scatter the laser light. Even in so-called filtered tap water some solid particles remain to scatter light, though the particle density is low. Using a TSI model 1090 tracker and a 20mw He-Ne laser over an order of magnitude variation in count rate was possible with the roughly filtered water used, depending on the gain setting of the photodetector. Typical voltage signals from the TSI 1090 tracker are shown in figure 3. Each oscilloscope trace represents 1 second of data obtained from the discharge of the nozzle. The time average velocity was nearly independent of spatial gradient along the vertical midplane and equal to 26cm/sec. Trace (a) is low gain 200 counts/sec (realizations of an internally verified velocity) signal; (b) is for a high gain setting 7000 counts/sec signal; and (c) is for the same gain setting as (a) except that bubble generating wire was located 400 wire diameters upstream from the LDA scattering volume. The hydrogen bubbles act as very effective light scatterers as seen by comparing traces (a) and (c). The noise of the signal using selective seeding, (c), is less than that using natural seeding uniformly distributed simply because the selective seeding from the 25μ dia. wire has reduced the effective measuring volume size. For purposes of averaging and spectral analysis, the signal obtained by

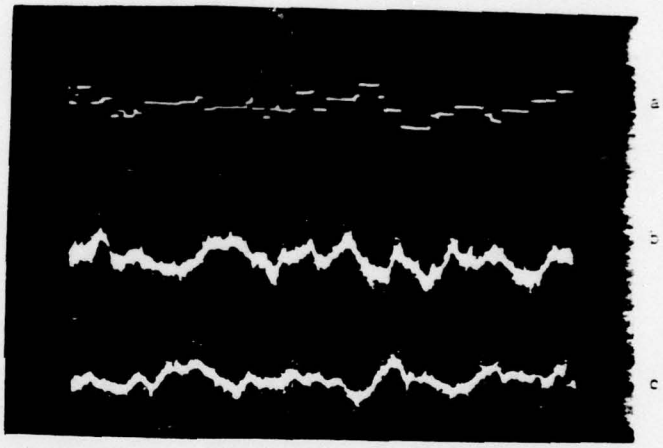

FIGURE 3: OSCILLOSCOPE TRACES OF VELOCITY IN THE FLUME USING LDA AT ABOUT 26 CM/SEC WITH (a) NATURAL SEEDING. 200 VELOCITY SAMPLES/SEC WERE MEASURED. (b) NATURAL SEEDING. 7000 VELOCITY SAMPLES/SEC WERE MEASURED (c) SELECTIVE SEEDING. THE BUBBLE WIRE WAS AT x/d = 400 AND 7000 VELOCITY SAMPLES/SEC. WERE MEASURED, INDICATING A VELOCITY DEFECT OF ABOUT 10%. WHEN THE BUBBLE WIRE WAS TURNED OFF, 200 SAMPLES/SEC. WERE MEASURED. ALL TRACES ARE 1 SEC. DURATION.

selective seeding can be treated in the same manner as the signal from natural seeding. Since the count rate is higher, it is often possible to examine higher frequency fluctuations in velocity using selective seeding than when using the natural background particles provided the hydrogen bubble can actually follow the velocity fluctuations in the flow.

VELOCITY FLUCTUATIONS

In order to determine how well the hydrogen bubbles actually followed the velocity fluctuations in the flow, the spectral response of the LDA velocity signal was compared with that obtained from a conven-

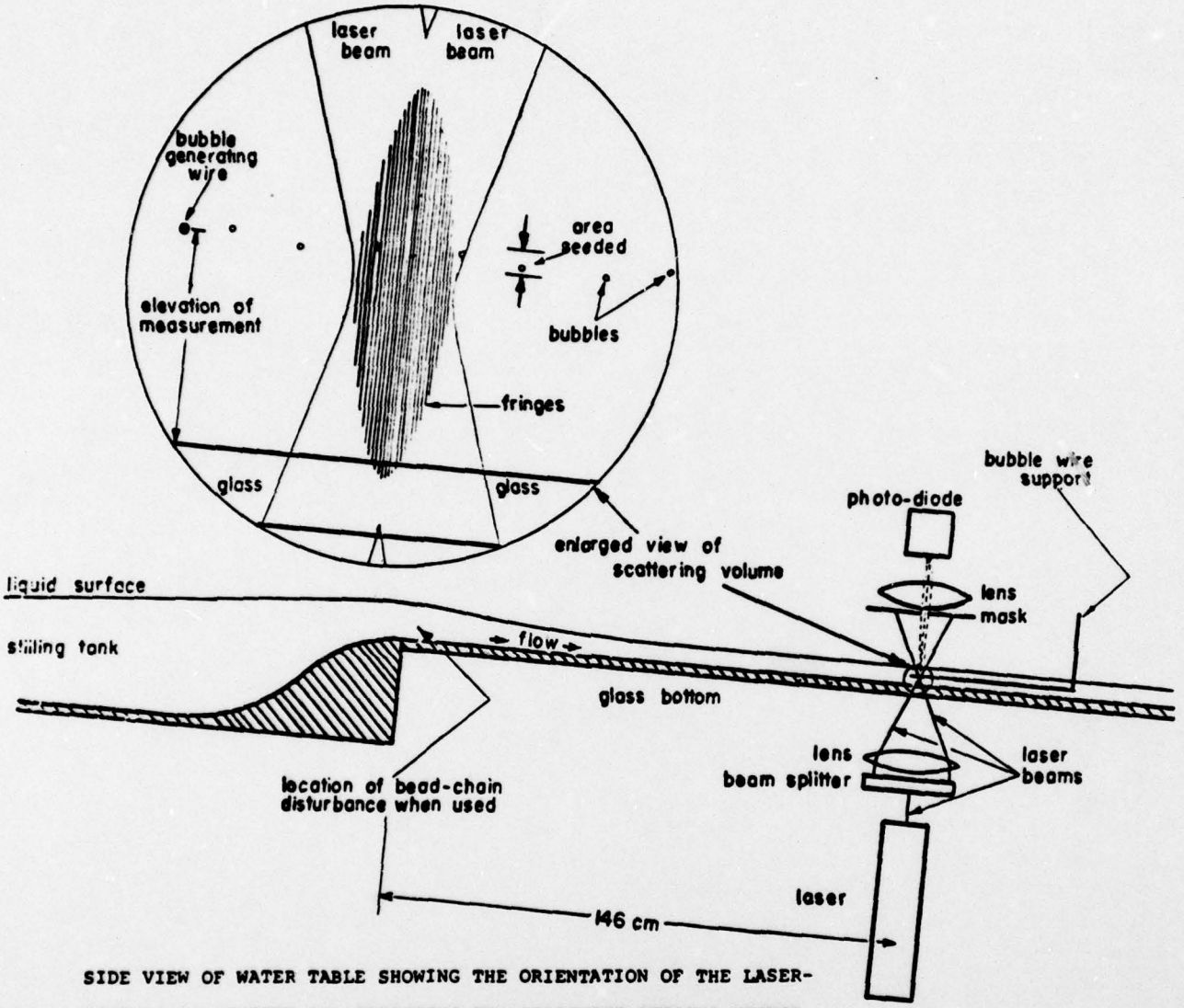

SIDE VIEW OF WATER TABLE SHOWING THE ORIENTATION OF THE LASER-DOPPLER ANEMOMETER AND DEPICTING THE SELECTIVE SEEDING METHOD.

FIGURE 4: SCHEMATIC OF WATER TABLE SHOWING THE LDA ARRANGEMENTS AND DEPICTING THE SELECTIVE SEEDING METHOD

tional hot-film anemometer. Two different flow situations were investigated, namely, that in the 15cm wide, free surface calibration flume and that on a free surface water table (figure 4) where high strain rate flows can be achieved (the velocity typically varied from 0 to 100 cm/sec across the approximately 2mm depth). In the calibration flume the maximum frequency of velocity fluctuations is on the order of 100Hz, while on the water table frequencies on the order of 300Hz are observed. It was for use on the water table that the selective seeding technique was first developed.

A conventional hot-film anemometer was used as the standard for measuring velocity fluctuations. The probe was a TSI model 1218 boundary layer probe (51μ diameter and quartz coated for use in water), and connected to a TSI model 1053B constant temperature anemometer bridge. The non-linear response was then used for measurement. The constant temperature system had a frequency response well into the kHz range, well beyond the frequency of observed flow fluctuations. In order to compare the frequency response of the various velocity measuring systems, the voltage output from the LDA tracker or the hot-film amplifier was processed

through a Tektronix 7L5 Spectrum Analyzer. Such a spectrum analyzer sweeps an adjustable narrow band digital filter across a given frequency range. The rate of sweep of the filter across the range is constant, hence the averaging time of the filtered signal near zero Hertz is less than the period of the center frequency. A turbulent velocity signal processed through such an instrument will naturally exhibit considerable fluctuation in the intensity at the zero frequency end of the spectrum which is an artifact of the electronics and would not be present if the sweep rate were lower.

The 7L5 Spectrum Analyzer was not designed to accept a dc signal from a high impedance source such as the TSI LDA system. Hence it was capacitor-coupled to an impedance matching operational amplifier of gain 1, resulting in attenuation of the signal below 4Hz. Figure 5 shows the output of the Spectrum Analyzer from a dc input on two amplitude scales used in the data presented. The noise level of the system is low and the output is flat above 10Hz. The oscilloscope output automatically displays the value of four adjustable parameters, three of which are useful in understanding the data to be presented. At the top center is the vertical intensity scale in millivolts R.M.S. per centimeter; bottom center is the width of the adjustable digital filter in Hertz; and at the bottom right is the abscissa scale in Hertz per centimeter, i.e. per grid space in the photograph. All data presented was measured using the 10Hz filter and covers the frequency range from zero to 500Hz.

In order to compare meaningfully the LDA output voltage fluctuations with those of a TSI-1053B-constant temperature hot-film anemometer, it is necessary to calibrate the hot-film system to have a voltage versus mean velocity curve for a given overheat ratio. This was done in the conventional way using the LDA system with natural seeding as the velocity standard. The local slope of the voltage-velocity curve was used as the linearized response of the hot-film system. The LDA system is linear in its response; however, a shift in separation in the optical beam splitter changes the slope of the voltage-velocity curve. By selecting a convenient mean velocity and beam separation it was possible to adjust the response ratio, R(22) or R(50) of the LDA output voltage to the hot-film output voltage to be nearly 2 or 4. Hence the display scale of the Spectrum

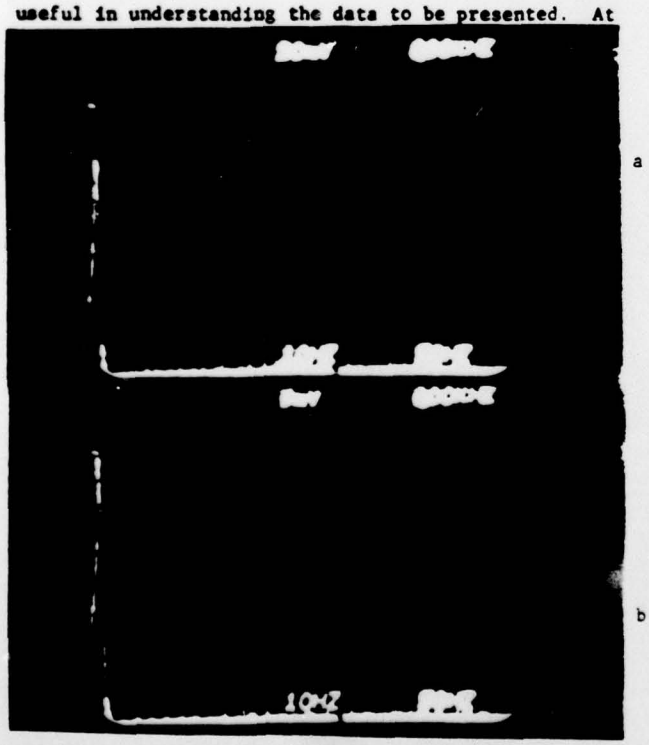

FIGURE 5: RESPONSE OF 7L5 SPECTRUM ANALYZER TO A DC SIGNAL AT DIFFERENT AMPLIFICATION. (a) 20mV/div. VERTICAL SPECTRAL AMPLITUDE (b) 5mV/div. VERTICAL SPECTRAL AMPLITUDE. THE HORIZONTAL SCALE RUNS FROM 0 TO 500Hz.

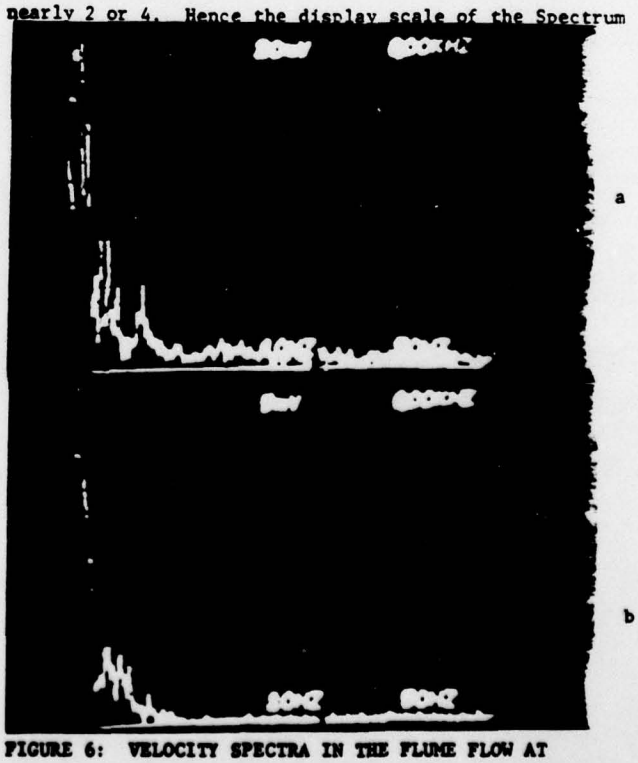

FIGURE 6: VELOCITY SPECTRA IN THE FLUME FLOW AT 40 CM/SEC. (a) LDA (50mm BEAM SEPARATION) - NATURAL SEEDING (b) HOT-FILM SENSOR. R(50) = 4.1 AND THE GAIN HAS BEEN ADJUSTED ON THE 7L5 BY A FACTOR OF 4 TO COMPARE WITH 6a. FOR COMPARISON WITH FIGURE 7, R(22) = 1.7.

frequency.

Spectra of the laminar flow velocity signal as measured by the selective seeding LDA method and by a hot-film probe are compared in figure 9.

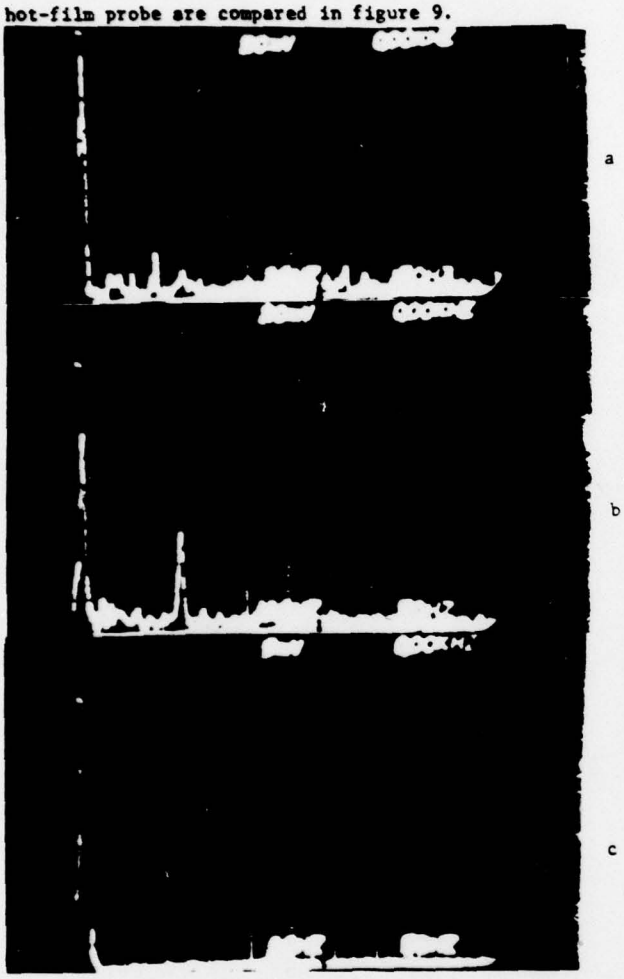

FIGURE 9: VELOCITY SPECTRA OF A LAMINAR WATER TABLE FLOW (FIGURE 8). (a) LDA (22), y = 0.066CM, y^+ = 25 (b) LDA (22), y = 0.046CM, y^+ = 18. WHEN 10 < y^+ < 25 FLOW EXCITATION OF A NATURAL FREQUENCY OF THE BUBBLE WIRE SUPPORT IS OFTEN OBSERVED BY HAVING A PEAK IN THE SPECTRUM AS SHOWN HERE AT ABOUT 120HZ.
(c) HOT-FILM SENSOR, y = 0.051CM, y^+ = 20.

Comparing the hot-film signal (figure 9c) with either LDA signal (figure 9a or 9b) shows the noise level of the selective seeding technique in such a flow. Laminar flow spectra at y^+ below 25 often exhibit a spike in intensity in the range of 100 to 200Hz. This artifact of the technique will be discussed in the next section.

Turbulent velocity spectra measured by the two techniques are presented in figure 10. The only significant difference between the hot-film measurements and the selectively seeded LDA measurements is the larger noise level at high frequency. From figure 9a it appears that the LDA noise is broad-band and in fact should be thought of as underlying the turbulent spectrum (figure 10a) also.

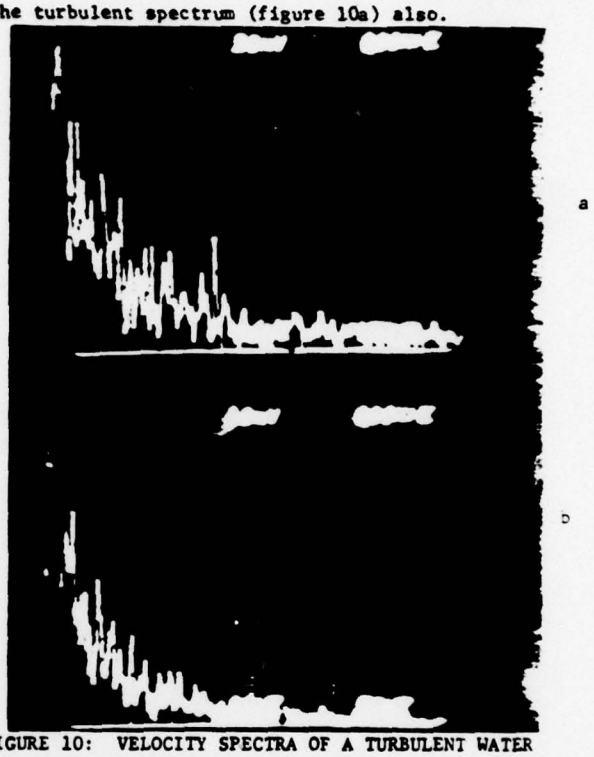

FIGURE 10: VELOCITY SPECTRA OF A TURBULENT WATER TABLE FLOW (FIGURE 8). (a) LDA (22), y = 0.147CM, y^+ = 67. (b) HOT FILM SENSOR, y = 0.155CM, y^+ = 67. R(22) = 1.9.

Except for the higher broad-band noise level, it has been demonstrated that the LDA selective seeding technique matches the performance of the hot-film anemometry. Bubbles from the 25μ dia. wire do follow the fluctuations in velocity and measure the average velocity when corrected by equ. (2) for the wire wake. Schraub et. al (1965) concluded from calculations that bubbles of the diameter used in these flows will in fact respond to fluctuations in the kiloHertz range; however, we have not found it necessary to experimentally verify the upper limit of the response capability of the system.

The selective seeding technique extends the usefulness of the LDA to flow regions of large velocity gradients and even reduces the noise level in cases where the mean gradient is zero or small. It has been invaluable to the authors in research involving dilute polymer solutions where the applicability of the hot-

Analyzer for the LDA was selected to be 2 or 4 times that of the hot-film so that the photographs of the spectra are nearly directly comparable.

The turbulent velocity spectrum in the calibration flume at 40 cm/sec velocity is shown in figure 6 as measured by the LDA system using natural seeding and by the hot-film anemometer. The comparison of the two spectra shows the noise level introduced above 150 Hz by the LDA system. The turbulent spectrum in the flume is concentrated primarily below 100 Hz.

Figure 7 shows a comparison of the same flow measured three different ways. The voltage sensitivity of the LDA is a factor of 2.4 less than it was in figure 6 since the beam separation was reduced from 50mm to 22mm to facilitate later comparisons with measurements on the water table.

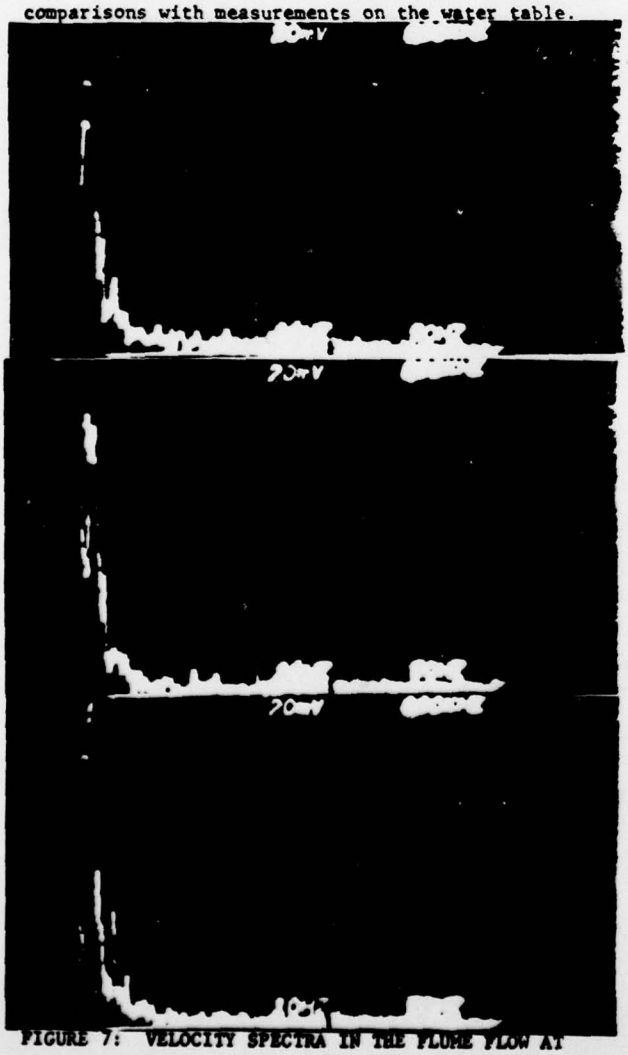

FIGURE 7: VELOCITY SPECTRA IN THE FLUME FLOW AT 38 CM/SEC USING LDA (22mm BEAM SEPARATION) WITH (a) NATURAL SEEDING (b) BUBBLE WIRE AT x/d = 100 (c) BUBBLE WIRE AT x/d = 500.

A comparison of figure 7(a) and 7(c) shows the lower noise level of the selective seeding technique (trace (c)) compared to the natural seeding at high frequencies. In addition, trace (c) at 500 diameters behind the wire more nearly mimics the very low frequency response of the natural seeding (a) without a wire present than does (b) taken only 100 diameters behind the bubble generation wire. The selective seeding technique, by easily allowing a high data count rate and by reducing the effective size of the scattering volume reduces the high frequency noise level and approaches the response of the hot-film probe. (Compare (6a and 7c)).

The flow in the flume is restricted to low frequencies; the flow on the free surface water table on the other hand has higher frequency components. The uncorrected velocity profiles of a laminar and a turbulent flow of water on the water table are shown in figure 8. Both of these profiles were measured using the selective seeding technique.

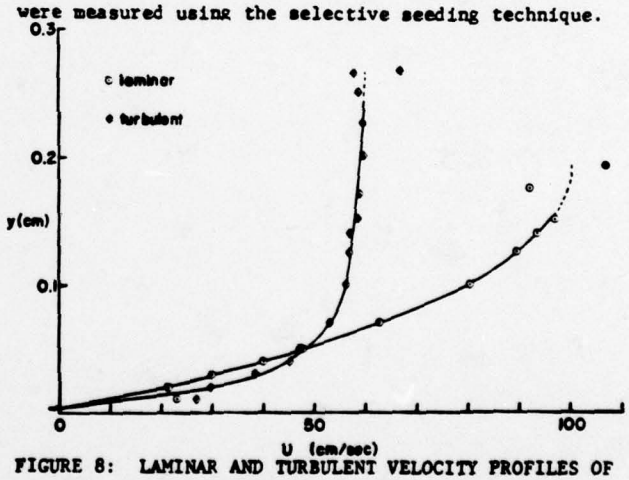

FIGURE 8: LAMINAR AND TURBULENT VELOCITY PROFILES OF A SHEAR FLOW OVER THE WATER TABLE AS MEASURED BY THE SELECTIVE SEEDING METHOD WITH x/d = 400. THE SOLID SYMBOLS ARE THE MEASURED VELOCITY OF POWDER SPRINKLED ON THE FREE SURFACE. THE ARROW AT 0.004CM INDICATES THE LOCATION OF THE WALL USING EXTRAPOLATION OF THE SLOPE DETERMINED BY THE WALL SHEAR STRESS AND THE LOWER DATA POINTS.

Comparison with standard LDA using natural seeding is impossible since the velocity gradient is too steep for such measurements. The bubble wire was aligned spanwise to the flow 400 diameters upstream of the optical crossing volume. Details are presented in the next section. The LDA output voltage was averaged by a continuously integrating op-amp. with an accuracy of 0.1% from dc to the several kiloHertz range in

film anemometry is doubtful at best.

COMMENTS ON USING THE TECHNIQUE

Experience indicated that great care must be exercised to maintain good quality measurements from the electrolysis bubbles. So, the wire was occasionally cleaned using a soft artist's paint brush to remove accumulated dirt (80% Pt 20% Ir proved more durable than 100% Pt and was supplied by Sigmund Cohn Corp., Mt. Vernon, N. Y.). Between brushings the wire was kept clean by changing the polarity frequently and slewing the voltage (80v to 300v) in order to drive off large gas bubbles. (As a side note, there were also unusual difficulties in using the hot-film sensor since the water could not be de-ionized. Ion rich water was needed to generate good electrolysis bubbles. To prevent severe drift, the sensor had to be brushed before each reading.)

When using the selective seeding technique in the environment of a high shear flow there are several points to keep in mind. The mean velocity profiles of figure 8 were obtained by moving the LDA system only once. Instead the bubble wire was moved, eliminating the need for a sophisticated LDA mount or the need to make continual optical adjustments. To facilitate data taking near a boundary, the optical scattering volume must be partially buried in the glass wall. Such measurements with selective seeding need no significant correction since the effective scattering volume is always completely within the flow. The data of figure 8 taken nearest to the wall show a definite tendency toward spuriously high velocities. In all likelihood, this was caused by driving the bubble wire into the wall. Since the wire support was flexible, the wire rose into the flow as the support was driven into the wall. While relative wire position was very accurately known (using a dial indicator on the support), the absolute elevation above the wall could only be roughly determined by finding the location of minimum velocity reading. Once a profile was obtained a better determination of the wall location was accomplished by extrapolating the profile to zero velocity, discounting those points which seemed spuriously high. For the water table data the fluid depth gave an independent method of determining the wall shear stress and hence the velocity profile's slope at the wall. Since the accuracy of this measurement was high, it was used to aid in locating the wall. In figure 8 the position of the wall was found to be at $y = 0.004$ cm and a small arrow indicates the location. Such an independent knowledge of the wall shear stress is frequently obtainable.

Another phenomenon related to the wire support can be seen in the spectrum of figure 9b. When measuring in laminar flows near the wall, discrete frequencies were often observed in the velocity spectrum. These appear to be caused by flow excitation of a natural frequency of the wire support. For the laminar profile of figure 8 such a spike was observed when $10 < y^+ < 25$.

Further investigation of figure 8 shows that as the wire nears the free surface, the velocity measurement is spuriously low. This is probably the result of the wire interacting with the surface primarily due to surface tension effects.

To obtain a surface velocity independently of selective seeding with electrolysis bubbles, talcum powder was sprinkled on the free surface and used as a preferential scattering agent with the LDA. While high density readings were not possible, approximate mean velocities were obtainable and are depicted as solid data points in figure 8. They appear to run about 11% higher than the extrapolation from the selective seeding data. From the analysis of the bubble velocity defect, a difference of about 6.5% from true free stream velocity was predicted. Since talcum powder is denser than water (sp. gr. 2.6-2.8) it will accelerate to a higher velocity as it moves down the incline of the water table and through the interaction of the film of talcum powder which forms on the surface, free surface boundary layers were expected. When lycopodium powder (density~ water) was used, the surface velocity measurement ran 1 or 2% less than when using talcum powder.

ACKNOWLEDGEMENTS

This work was supported in part by the Fluid Mechanics Program of the National Science Foundation, Grant NSF-ENG77-01478, The Division of Applied Sciences, Harvard University, Cambridge, Mass. 02138 and the USA Office of Naval Research.

REFERENCES

Bertschy, J. R. & Abernathy, F. H. (Aug. 31-Sept. 2, 1977) "Modifications to laminar and turbulent boundary layers due to the addition of dilute polymer solutions" BHRA Fluid Engineering, 2nd Int. Conf. on Drag Reduction.

Grass, A. J. (1971) "Structural features of turbulent flow over smooth and rough boundaries" J. Fluid Mech. 50, 233-255.

Schlichting, H. (1968) Boundary-Layer Theory, 6th Ed. McGraw-Hill, p. 694.

Schraub, F. A., Kline, S. J., Henry, J. Runstadler, P. W. Jr., Littel, A. (1965) "Use of Hydrogen Bubbles for Quantitative Determination of Time-Dependent Velocity Fields in Low-Speed Water Flows" J. Basic Eng'g, ASME Trans. Series D, 87, 429.

Shapiro, A. H. (1972) Illustrated Experiments in Fluid Mechanics, MIT Press.

Tritton, D. J. (1959) "Experiments on the flow past a circular cylinder at low Reynolds numbers" J. Fluid Mech. 6, 547-567.